

5. DATA REPORT: TEXTURAL VARIATION OF UNITS 1256C-18 AND 1256D-1 LAVA POND, WITH SPECIAL REFERENCE TO RECRYSTALLIZATION OF THE BASE OF UNIT 1256C-18¹

Susumu Umino²

INTRODUCTION

Hole 1256C was cored 88.5 m into basement, and Hole 1256D, the deep reentry hole, was cored 502 m into basement during Ocean Drilling Program Leg 206. Hole 1256D is located ~30 m south of Hole 1256C (Wilson, Teagle, Acton, et al., 2003). A thick massive flow drilled in both holes, Units 1256C-18 and 1256D-1, consists of a single cooling unit of cryptocrystalline to fine-grained basalt, interpreted as a ponded lava, 32 m and at least 74.2 m thick, respectively. This ponded flow gives us a unique opportunity to examine textural variations from the glassy, folded crust of the lava pond recovered from the top of Unit 1256C-18 through the coarse-grained, thick massive lava body to the unusually recrystallized and deformed base cored in Unit 1256C-18. Some detailed descriptions of the textures and grain size variations through the lava pond (Units 1256C-18 and 1256D-1), with special reference to the recrystallization of the base of Unit 1256C-18, are presented here.

METHODS

A total of 124 samples from Unit 1256C-18 and 47 samples from Unit 1256D-1 were made into thin sections for conventional microscopic and scanning electron microscopic observations. Representative

¹Umino, S., 2007. Data report: textural variation of Units 1256C-18 and 1256D-1 lava pond, with special reference to recrystallization of the base of Unit 1256C-18. In Teagle, D.A.H., Wilson, D.S., Acton, G.D., and Vanko, D.A. (Eds.), *Proc. ODP, Sci. Results*, 206: College Station, TX (Ocean Drilling Program), 1–32.
doi:10.2973/odp.proc.sr.206.007.2007

²Institute of Geosciences, Shizuoka University, Ohya 836, Suruga-ku, Shizuoka 422-8529, Japan.
sesumin@ipc.shizuoka.ac.jp

textures are shown in Figure F1. Among these thin sections, 58 from Unit 1256C-18 and 47 from Unit 1256D-1 were examined to determine the average maximum grain size of the groundmass plagioclase and augite. The measurement procedures followed those of Shipboard Scientific Party (1992) and Umino (1995), except for measurements on the recrystallized base from Hole 1256C, and are reproduced here. Twelve circular areas of $\sim 13 \text{ mm}^2$ were chosen from each thin section. Selection of measured areas was made so as not to overlap each other and to minimize the area occupied by phenocrysts. The length and width of the largest crystals of plagioclase and augite were measured under the microscope. The longest extensions of plagioclase and augite are measured as the length, and the widths are measured perpendicular to elongation at the widest portion of the crystals. A plagioclase grain is usually composed of twinned crystals, which are often displaced along the twin planes and terminate at different positions. In such a case, only the longer single crystal was measured as the length. This measurement was repeated in every circle. The largest and smallest values of the 12 measurements were excluded. The remaining 10 values were averaged as the maximum grain size. For recrystallized samples from the base of Unit 1256C-18, the grain size was determined as follows: the largest 10 grains of plagioclase, augite, and magnetite were chosen from an area of $\sim 40 \text{ mm}^2$ under the microscope, and their lengths and widths were measured as described above and averaged to give the average maximum grain size. The results of the measurement are given in Tables T1 and T2 and are shown in Figure F2.

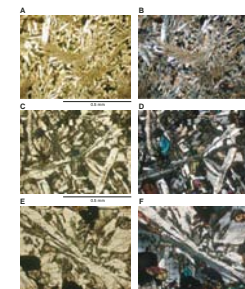
Mineral compositions of selected samples from the recrystallized base of Unit 1256C-18 were determined by a JEOL JXA-733 electron probe microanalyzer (EPMA) of the Center for Instrumental Analysis, Shizuoka University. Corrections were made according to Bence and Albee (1968), using α factors of Nakamura and Kushiro (1970). Accelerating voltage was 15 kV and beam current was $1.2 \times 10^{-8} \text{ A}$. Analytical results are listed in Table T3, and plagioclase and clinopyroxene compositions are shown in Figure F9.

RESULTS

Textures of Lava Pond

In Hole 1256C, where an almost complete succession of the lava pond was recovered, the basalt is a macroscopically homogeneous, massive microcrystalline to fine-grained lava with a coarse variolitic to intergranular texture, apart from the uppermost 0.7 m and the basal 1.7 m. Neither the top nor the base of the lava pond were recovered in Hole 1256D. Although Unit 1256D-1 is more than twice as thick as Unit 1256C-18, the lava is similar to Unit 1256C-18 both in hand specimen and under the microscope, consisting of microcrystalline to fine-grained basalt with similar groundmass textures. The basalt lava has 0.5–11 vol% olivine with only traces of plagioclase and clinopyroxene as phenocrysts. The groundmass consists of plagioclase and augite with a subordinate amount of magnetite and a small amount of pigeonite and with or without glass. Besides the folded surface crust of the lava pond in the uppermost 0.7 m and the recrystallized base of Unit 1256C-18, the massive lava contains interstitial mesostasis of quartz-albite granophytic to vermicular intergrowths, quartz, clinopyroxene, apatite,

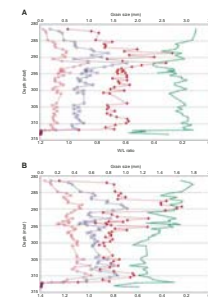
F1. Variety of variolitic textures, p. 8.



T1. Average maximum grain sizes, p. 26.

T2. Average maximum grain sizes of recrystallized base, p. 28.

F2. Downhole variations of plagioclase and augite grain sizes, p. 9.



T3. Mineral compositions, p. 29.

and dendritic to skeletal magnetite with ilmenite lamellae. Granophyric veins and pods may also appear as late-stage magmatic products.

A common groundmass texture prevails through almost all basalt lava samples from Site 1256, which consists mainly of clinopyroxene and plagioclase ± disseminated magnetite. Both clinopyroxene and plagioclase are radially arranged to form spheroidal or fan-shaped crystal aggregates, finer-grained varieties of which have been traditionally called varioles (Fig. F1). MacKenzie et al. (1982) used the term “varioles” for fanlike varieties and “spherulites” for spheroidal crystal aggregates irrespective of the constituent mineral species and the host rock compositions. However, spherulites are traditionally used for those consisting essentially of feldspars in felsic rocks, and similar textures that occur in mafic rocks are termed varioles. I prefer the conventional usage of varioles but broaden its definition to include fan-shaped varieties of prismatic to platy crystal aggregates of clinopyroxene and plagioclase similar to spheroidal varioles.

Devitrification of a quenched flow surface begins within a few millimeters of the surface as patches of fine cervicon-plumose crystallites, predominantly clinopyroxene, form. Both the number density of the crystallite patches and the crystal density in individual patches rapidly increase toward the flow interior and occupy the entire groundmass with dark brownish varioles that are barely translucent under the microscope. Many varioles near the front of the dense variole zone have tiny microlites of plagioclase or olivine in their cores and are elongated to the orientation of the microlites, showing that they nucleated on the preexisting microlites. Typical varioles occur within a zone 1–2 cm beneath the surface and are composed of very fine grained fibrous aggregates of clinopyroxene with minor amounts of thin plagioclase laths. Tiny magnetite grains may be disseminated in and between the pyroxene-plagioclase aggregates. Samples taken further into the interior of lava flows show preferential growth of clinopyroxene over plagioclase where clinopyroxene forms larger curved sheaves of acicular crystals with the intergrown plagioclase laths much less abundant (fine varioles) (Fig. F1A, F1B). As the groundmass crystals coarsen, both plagioclase and clinopyroxene thicken to form more stubby and prismatic crystals. Eventually the growth rate of plagioclase and clinopyroxene is reversed, and further into the interiors of thick massive flows plagioclase becomes skeletal to platy with bowtie-like crystals larger than clinopyroxene forming subhedral to euhedral prisms broadening toward the exterior of varioles (medium varioles). There is also a transitional type that has both plagioclase and clinopyroxene crystals similarly developed in the cores of thick sheet flows and massive lava.

Further development of variolitic texture is only observed in the thick massive lavas from Units 1256C-18 and 1256D-1, which are interpreted as a lava pond by the Leg 206 Shipboard Scientific Party (Wilson, Teagle, Acton, et al., 2003). Stubby clinopyroxene coagulates near the center of a larger plagioclase crystal to form a hub from which a few crystals of platy plagioclase radiate (coarse varioles) (Fig. F1C, F1D). The variole hub is usually composed of several clinopyroxene crystals, but in some cases only one or two clinopyroxene crystals showing a patchy extinction pattern are intergrown with radiating plagioclase crystals. This suggests that gradual coalescence and reorientation of several clinopyroxene crystals into a single continuous crystal took place in the slowly cooling lava. An extremely developed variety can be seen in the coarsest part of the lava pond, where large plagioclase crystals poikiliti-

cally enclose clinopyroxene crystals with different crystallographic orientations (Fig. F1E, F1F).

The distribution, morphology, and size of varioles appear to change in response to the distance from the chilled margin, the main factor that determines the degree of undercooling. In the core of the lava pond, fine and medium varioles tend to form as randomly spaced isotropic spheroids, consistent with crystallization under static conditions. However, varioles beneath the deforming surface crust and recrystallized base of the lava pond are flattened and oriented subparallel to the shear plane or disintegrated into bands of granular pyroxene and platy plagioclase intercalated with flattened variole-rich bands.

Downhole Variations in Grain Size

In Unit 1256C-18, the average maximum plagioclase grain size rapidly increases with depth in the upper 2 m from the surface of the lava pond (Fig. F2A) and then shows stepwise increases up to 2.7 and 0.53 mm in length and width, respectively, at 289 meters below seafloor (mbsf). From this depth to 293 mbsf, the plagioclase grain size widely fluctuates from 1.4 to 2.6 mm in length (0.7–1.8 mm in diameter of a circle with an equivalent area to the crystal [EQD]). Below this depth range, the plagioclase grain size remains almost constant (1.56 ± 0.21 mm in length and 0.83 ± 0.16 mm in EQD) with little variation. The width/length ratio of plagioclase varies in accordance with the size variations. The ratio remains low (0.11–0.12) in the uppermost 2 m of the unit but increases quickly to 0.35, from which it varies between 0.13 and 0.41 to 293 mbsf. Below this depth, the width/length ratio remains almost constant at ~0.23 but shows an overall slight decrease down-hole. As the width/length ratio indicates, the zone of coarse-grained plagioclase at 289–293 mbsf has larger, more equant plagioclase than elsewhere in Unit 1256C-18.

The average maximum augite grain size shows a similar pattern to plagioclase, and the peak in grain size also occurs at 289 mbsf (Fig. F2B). The width/length ratio of augite shows different variations from those of plagioclase, especially in the lower half of the unit. Below the zone of coarse-grained augite, the width/length ratio further increases to 0.64 at 301 mbsf and then remains constant at 0.56 ± 0.05 to 310 mbsf. The coarse augite zone is due to the abundant elongate prismatic augite crystals with pigeonite core that have low width/length ratios. The lower half of Unit 1256C-18 has some elongate augite prisms; however, they are much less abundant than the stubby to equant augite crystals.

Plagioclase and augite from Unit 1256D-1 generally show similar variations in maximum grain size as Unit 1256C-18 (Fig. F2C, F2D). Unlike Hole 1256C, the largest grain size occurs near the top of the unit (282 mbsf), which may be ascribed to the unrecovered uppermost part of the lava pond in Hole 1256D. However, the width/length ratio of plagioclase has the highest value of 0.36 below the depth of the peak maximum grain size and then rapidly decreases to 0.18, as in Hole 1256C. The largest plagioclases at 282 mbsf in Hole 1256D form long but thin platy crystals, suggestive of rapid growth under a large degree of undercooling.

The coarse-grained plagioclase and augite zones in Holes 1256C and 1256D are enriched in incompatible elements and coincide with the high magnetic susceptibilities (Wilson, Teagle, Acton, et al., 2003), which are explained by the concentration of differentiated melt in the

upper part of the massive lava body. This indicates that the lava body solidified mainly from the bottom and the residual melt became more enriched in incompatible elements and volatiles as it accumulated into the upper part of the body, promoting the growth of large grains of plagioclase and augite. Such a bottom-up solidification of a lava body differs from that of subaerial inflating sheet flows (Kauahikaua et al., 1998), but is well known from observations based on direct drilling into solidifying lava lakes in Hawaii (Helz et al., 1989).

Recrystallization of the Base of Unit 1256C-18

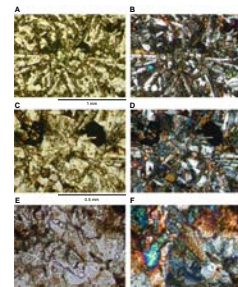
The lowermost 1.6-m-thick core of Unit 1256C-18 is an aphyric cryptocrystalline basalt with an unusual groundmass texture of equigranular clinopyroxene and magnetite with sparse plagioclase laths (Fig. F3, F4). The sample from the deepest portion of Unit 1256C-18 (Sample 206-1256C-11R-7, 130–133 cm) has a groundmass with a variolitic texture, where varioles 0.1–0.3 mm in diameter are composed of slightly elongate, subround clinopyroxene crystals 10–15 µm in length aligned in curved lines radiating from the center of varioles and uncommon plagioclase laths 10–40 µm in length with disseminated granular magnetite (Fig. F4S–F4X). Unlike cryptocrystalline basalt with similar fine variolitic textures and grain sizes, skeletal magnetite is less common than equant crystals and clinopyroxene crystals are granular instead of fibrous-dendritic forms. In contrast, plagioclase tends to retain elongate skeletal forms. Plagioclase phenocrysts and larger laths have an embayed subhedral outline where original plagioclase is disintegrated into tiny (<10 µm) granular crystals of plagioclase. Recrystallization is more completely advanced upward, and at 1 m above the base of Unit 1256C-18 (Sample 206-1256C-11R-7, 33–36 cm), clinopyroxene is completely recrystallized and magnetite barely preserves elongate dendritic forms (Fig. F4G–F4L). At 1.2 m above the base (Sample 206-1256C-11R-7, 9–12 cm), clinopyroxene in the original groundmass is completely recrystallized into equant equigranular neoblasts and magnetite scarcely shows the remnant of skeletal crystal forms. Nevertheless, the igneous variolitic texture is still identifiable from the alignment of granular clinopyroxene and elongate blebs of plagioclase. This is especially true for larger varioles, suggesting that recrystallization is strongly dependent on the original grain size and mineral species (Figs. F5, F6, F7). Figure F8 shows the groundmass grain size variations through the recrystallized base of Unit 1256C-18. Both clinopyroxene and magnetite show steady increases in grain size toward the main body of the lava pond. This can be explained if the driving force of recrystallization was heat supplied from the thick ponded lava above. In contrast, plagioclase does not show any trend of grain size variation with depth, which is consistent with the view that plagioclase retains primary igneous textures and is most resistive to recrystallization.

Coarser-grained late magmatic veins are seen in interval 206-1256C-11R-7, 20–110 cm (see Figs. F4, F5, F6). These veins are composed of plagioclase, quartz, magnetite, brownish clinopyroxene with pale to dark green rims, and granophytic to vermicular intergrowths of sodic plagioclase and quartz. This is an identical mineral assemblage to the mesostasis in the fine-grained basalt of the massive lava pond. Samples 206-1256C-11R-7, 33–36 cm, and 11R-7, 47–50 cm, show progressive recrystallization of more intensely deformed vein minerals than later, less-deformed veins with chilled margins against the host basalt (Fig. F4G–F4L). Earlier veins are more progressively recrystallized into

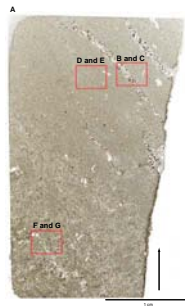
F3. Core image of the recrystallized base of Unit 1256C-18, p. 11.



F4. Photomicrographs showing textural variations, p. 12.



F5. SEM images of Sample 206-1256C-11R-7, 47–50 cm, p. 16.



F6. SEM images of Sample 206-1256C-11R-7, 76–79 cm, p. 18.



equigranular neoblasts and show evidence of subsolidus intracrystalline deformation such as undulose extinction and kink bands. This, together with the undulating margins of the veins, suggests that either the deformation took place under hypersolidus conditions or the rate of replacement of deformed crystals with neoblasts always exceeded the rate of intracrystalline deformation. Examination of core sections cut subparallel to and normal to the core show that the deformed veins have sheath foldlike structures.

Mineral Chemistry

Plagioclase and clinopyroxene in three stratigraphically different samples from the recrystallized base of Unit 1256C-18 were analyzed by EPMA and are shown in Figure F9 and Table T3. All samples have minimal differences in ranges of An mol% of plagioclase and Mg# of clinopyroxene and show the same overall differentiation trend. Plagioclase shows a slight enrichment in FeO with decreasing An from 80 to 60 and a wide scatter in FeO from 0.7 to 2.1 wt% at lower An contents. Most plagioclase phenocryst cores are An_{80–68}, whereas rims have a similar range in composition to the groundmass laths and are as low as An₄₃. Plagioclase in veins mostly plots in the same range as the phenocryst rims and groundmass laths, although some grains have significantly lower An contents (An_{43–6}) (Table T3). Recrystallized plagioclase neoblasts plot in the lower An range (An_{50.6–52.3}) of the groundmass plagioclase.

Clinopyroxene phenocrysts are exclusively augite, whereas crystals in the groundmass and veins plot in both augite and pigeonite fields (Fig. F9B). Some have Wo content as low as hypersthene; however, no orthopyroxene was identified under the microscope. Although the number of analyses of phenocrysts is few, they show three distinct clusters (Fig. F9C, F9D): two cores with high Mg# (~82), two cores and three rims with low Mg# (58–66), TiO₂ (0.5–0.8 wt%), and Al₂O₃ (1.2–1.5 wt%), and one core with low Mg# (59) and high TiO₂ (>1.3 wt%) and Al₂O₃ (2.4 wt%). The groundmass augite overlaps the latter two and extends to lower Mg#. Augite in veins also plots in the same range as the low-Mg# phenocrysts and the groundmass crystals. Pigeonite in the groundmass and veins shows lower Mg#, TiO₂, and Al₂O₃ contents than the majority of augite, and it appears to plot on the same trend together with those augite. Recrystallized augite neoblasts have Mg# 59.3–61.6, TiO₂ 0.61–0.84 wt%, and Al₂O₃ 1.26–1.61 wt%, which are within the groundmass compositions.

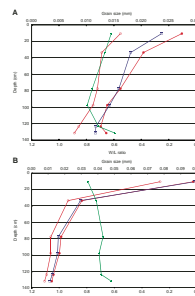
ACKNOWLEDGMENTS

I would like to thank the crew and technical staff of the *JOIDES Resolution* and the Leg 206 Shipboard Science Party for sampling and data acquisition. Thanks also to Hideki Mori for making polished thin sections for EPMA analyses. The manuscript benefited from critical reviews by Sumio Miyashita and Hiroaki Sato. This research used samples and/or data provided by the Ocean Drilling Program (ODP). ODP is sponsored by the U.S. National Science Foundation (NSF) and participating countries under management of Joint Oceanographic Institutions (JOI), Inc.

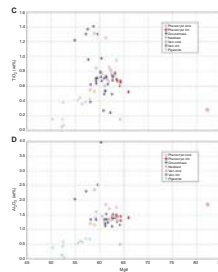
F7. SEM images of Sample 206-1256C-11R-7, 96–100 cm, p. 20.



F8. Grain size variations of groundmass crystals in Hole 1256C, p. 22.



F9. Mineral compositions of samples, p. 24.



REFERENCES

- Bence, A.E., and Albee, A.L., 1968. Empirical correction factors for the electron microanalysis of silicates and oxides. *J. Geol.*, 76:382–403.
- Helz, R.T., Kirschenbaum, H., and Marinenco, J.W., 1989. Diapiric transfer of melt in Kilauea Iki lava lake, Hawaii: a quick, efficient process of igneous differentiation. *Geol. Soc. Am. Bull.*, 101(4):578–594. doi:[10.1130/0016-7606\(1989\)101<0578:DTOMIK>2.3.CO;2](https://doi.org/10.1130/0016-7606(1989)101<0578:DTOMIK>2.3.CO;2)
- Kauahikaua, J., Cashman, K.V., Mattox, T.N., Heliker, C.C., Hon, K.A., Mangan, M.T., and Thornber, C.R., 1998. Observations on basaltic lava streams in tubes from Kilauea volcano, island of Hawai'i. *J. Geophys. Res.*, 103(B11):27303–27324. doi:[10.1029/97JB03576](https://doi.org/10.1029/97JB03576)
- MacKenzie, W.S., Donaldson, C.H., and Guilford, C., 1982. *Atlas of Igneous Rocks and their Textures*: Harlow, England (Longman).
- Nakamura, Y., and Kushiro, I., 1970. Compositional relations of coexisting orthopyroxene, pigeonite, and sugite in a tholeiitic andesite from Hakone volcano. *Contrib. Mineral. Petrol.*, 26(4):265–275. doi:[10.1007/BF00390075](https://doi.org/10.1007/BF00390075)
- Shipboard Scientific Party, 1992. Site 504. In Dick, H.J.B., Erzinger, J., Stokking, L.B., et al., *Proc. ODP, Init. Repts.*, 140: College Station, TX (Ocean Drilling Program), 37–200.
- Umino, S., 1995. Downhole variations in grain size at Hole 504B: implications for rifting episodes at mid-ocean ridges. In Erzinger, J., Becker, K., Dick, H.J.B., and Stokking, L.B. (Eds.), *Proc. ODP, Sci. Results*, 137/140: College Station, TX (Ocean Drilling Program), 19–34.
- Wilson, D.S., Teagle, D.A.H., Acton, G.D., et al., 2003. *Proc. ODP, Init. Repts.*, 206: College Station, TX (Ocean Drilling Program). doi:[10.2973/odp.proc.ir.206.2003](https://doi.org/10.2973/odp.proc.ir.206.2003)

Figure F1. Variety of variolitic textures. A, B. Very fine varioles consisting of curled plumose clinopyroxene intervened with thin plagioclase laths (Sample 206-1256C-8R-5, 21–24 cm). C, D. Medium varioles with platy plagioclase more developed than granular-prismatic clinopyroxene (Sample 206-1256C-8R-6, 4–7 cm). E, F. Coarse varioles consisting of stubby-platy plagioclase enclosing radially arranged clinopyroxene (Sample 206-1256C-9R-5, 58–61 cm).

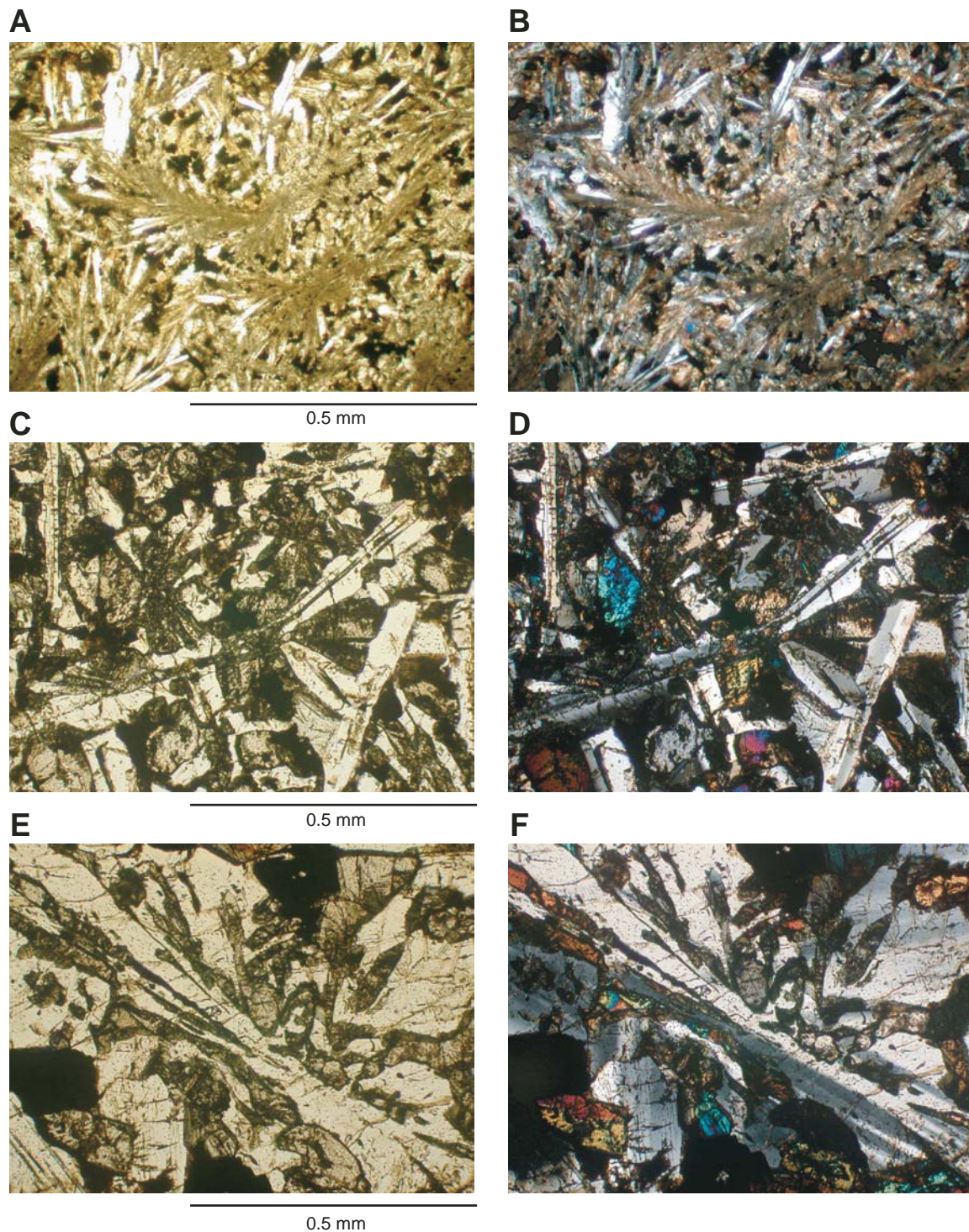


Figure F2. Downhole variations of (A) plagioclase and (B) augite grain sizes in Unit 1256C-18. Solid circles = average maximum length, open circles = average maximum width, squares = diameter of a circle with an equivalent area to the crystal, crosses = maximum width/length (W/L) ratio. (Continued on next page.)

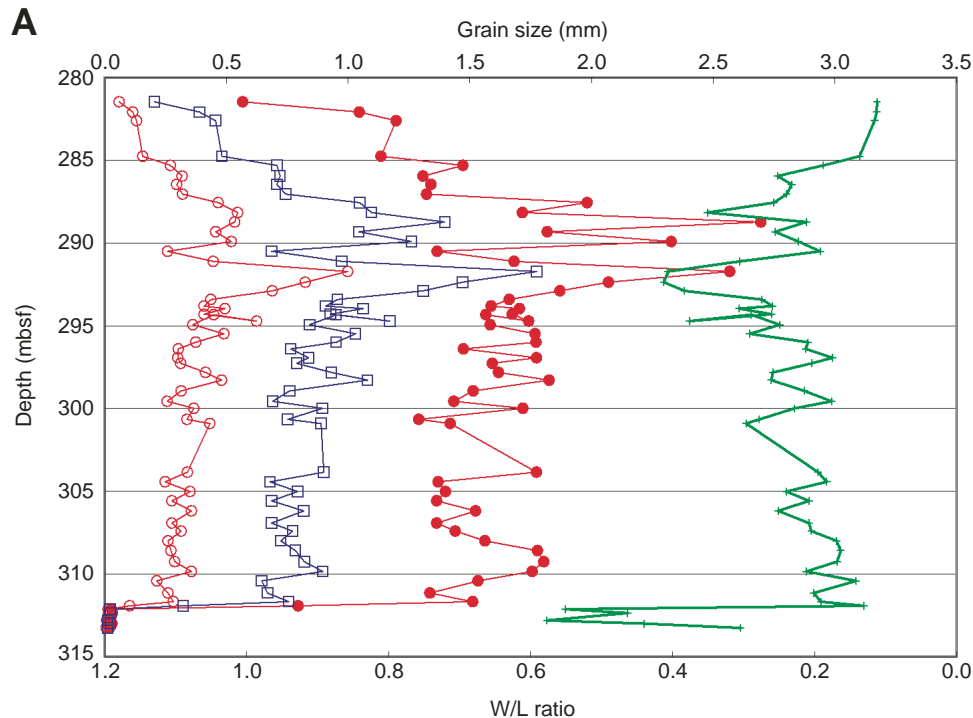
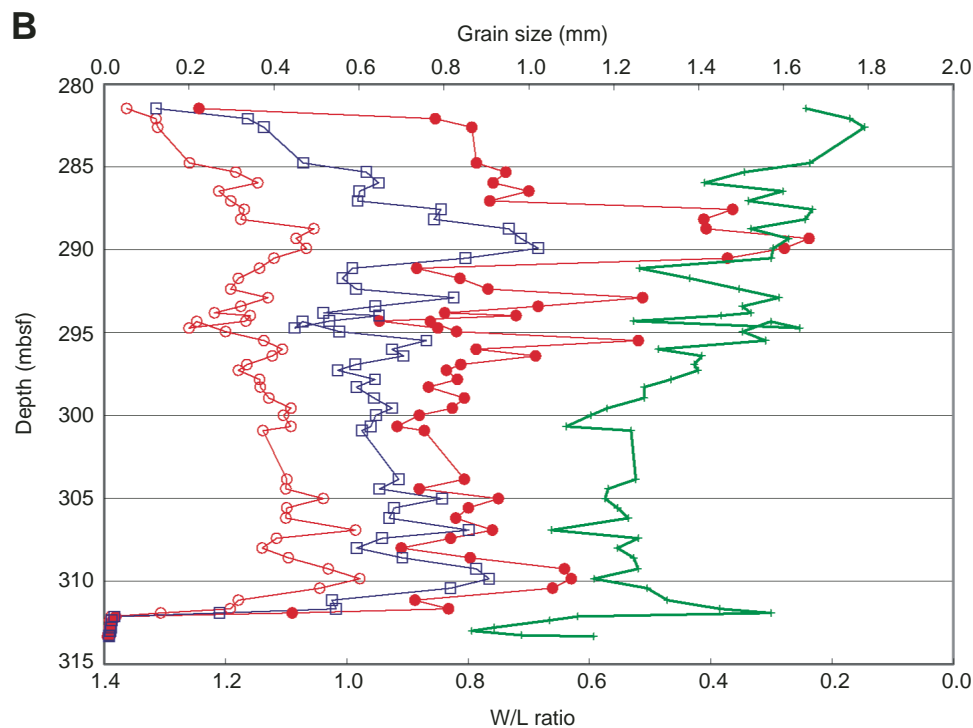
A**B**

Figure F2 (continued). Downhole variations of (C) plagioclase and (D) augite grain sizes in Unit 1256D-1. Solid circles = average maximum length, open circles = average maximum width, squares = diameter of a circle with an equivalent area to the crystal, crosses = maximum width/length (W/L) ratio.

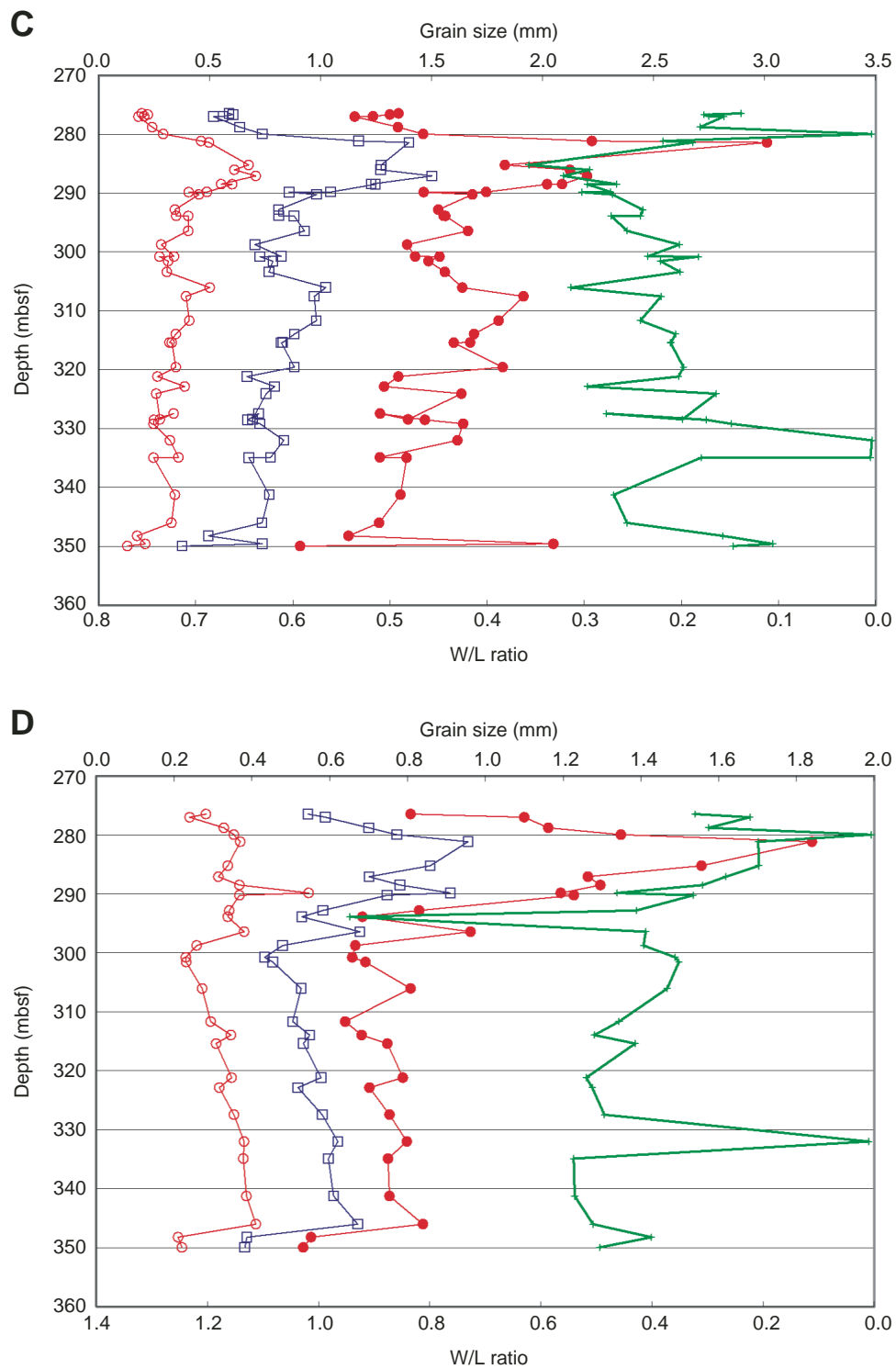


Figure F3. Core image of the recrystallized base of Unit 1256C-18 with sample locations for thin sections (rectangles on the core image) showing textural variations. Photomicrographs of selected samples are shown in Figure F4, p. 12, of which positions are shown by small rectangles on the thin section images.

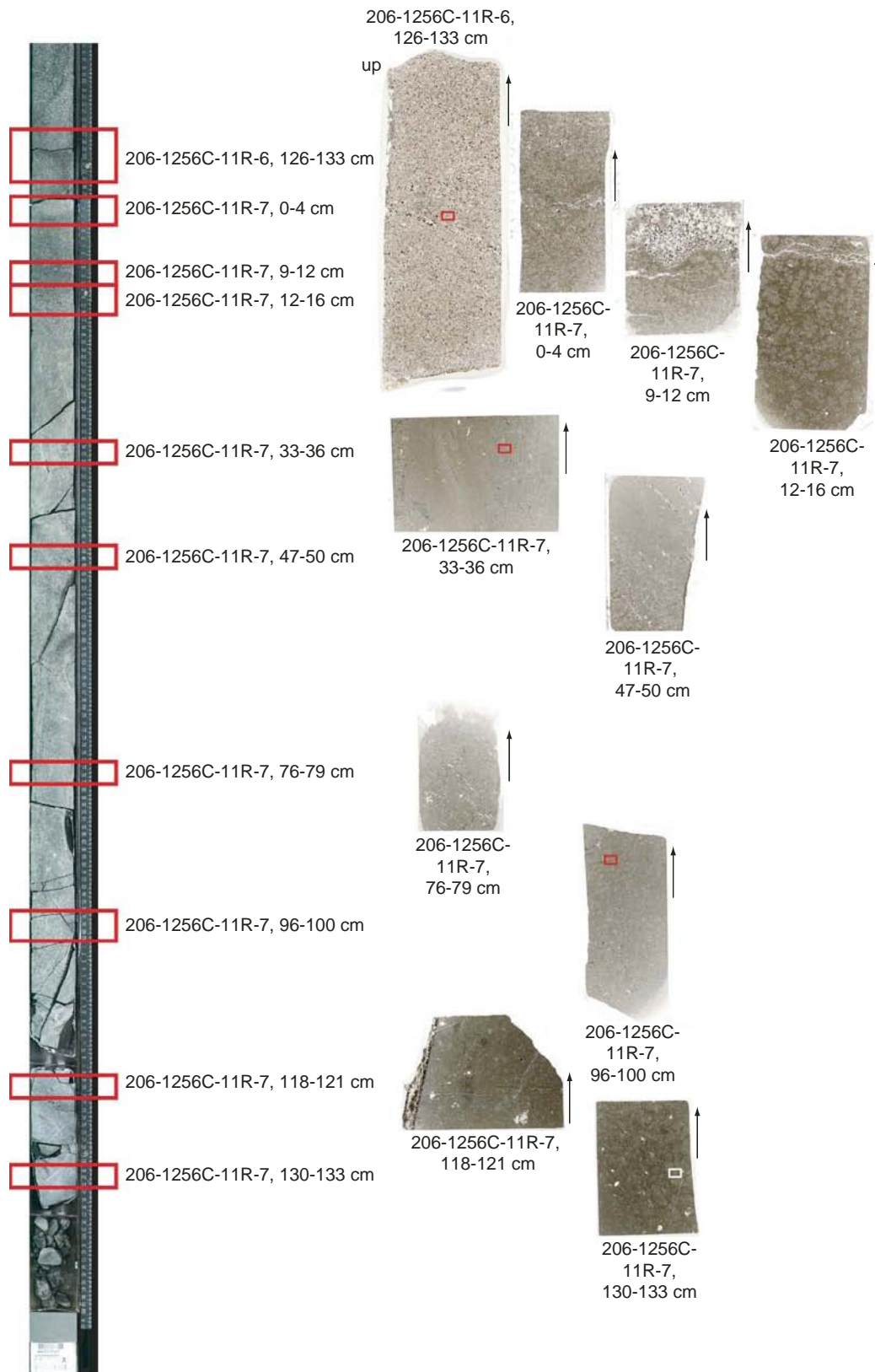


Figure F4. Selected photomicrographs of (A–F) Sample 206-1256C-11R-6, 126–133 cm, showing textural variations of the recrystallized base of Unit 1256C-18. (Continued on next three pages.)

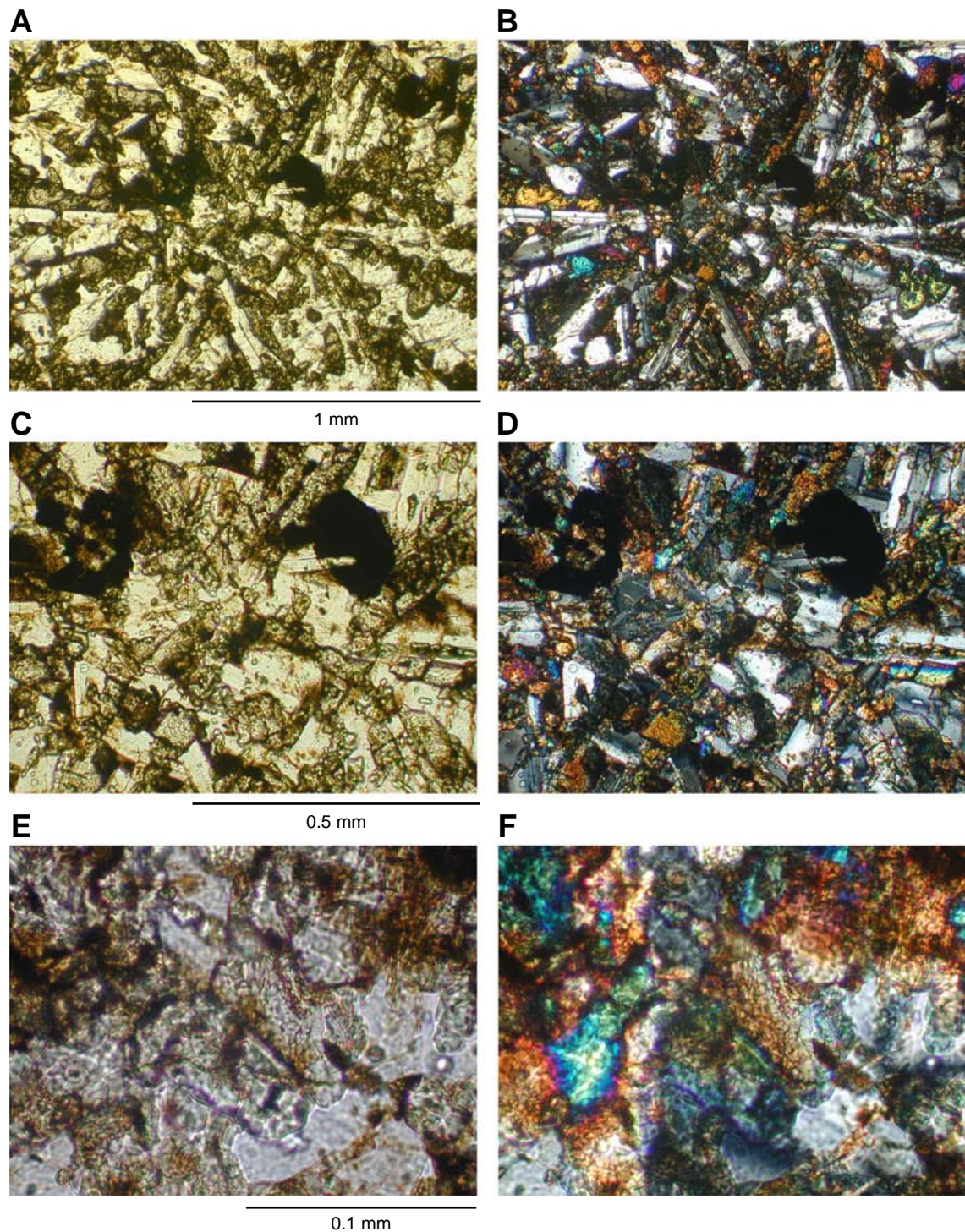


Figure F4 (continued). Selected photomicrographs of (G, H) Sample 206-1256C-11R-7, 47–50 cm, and (I–L) Sample 206-1256C-11R-7, 33–36 cm, showing textural variations of the recrystallized base of Unit 1256C-18.

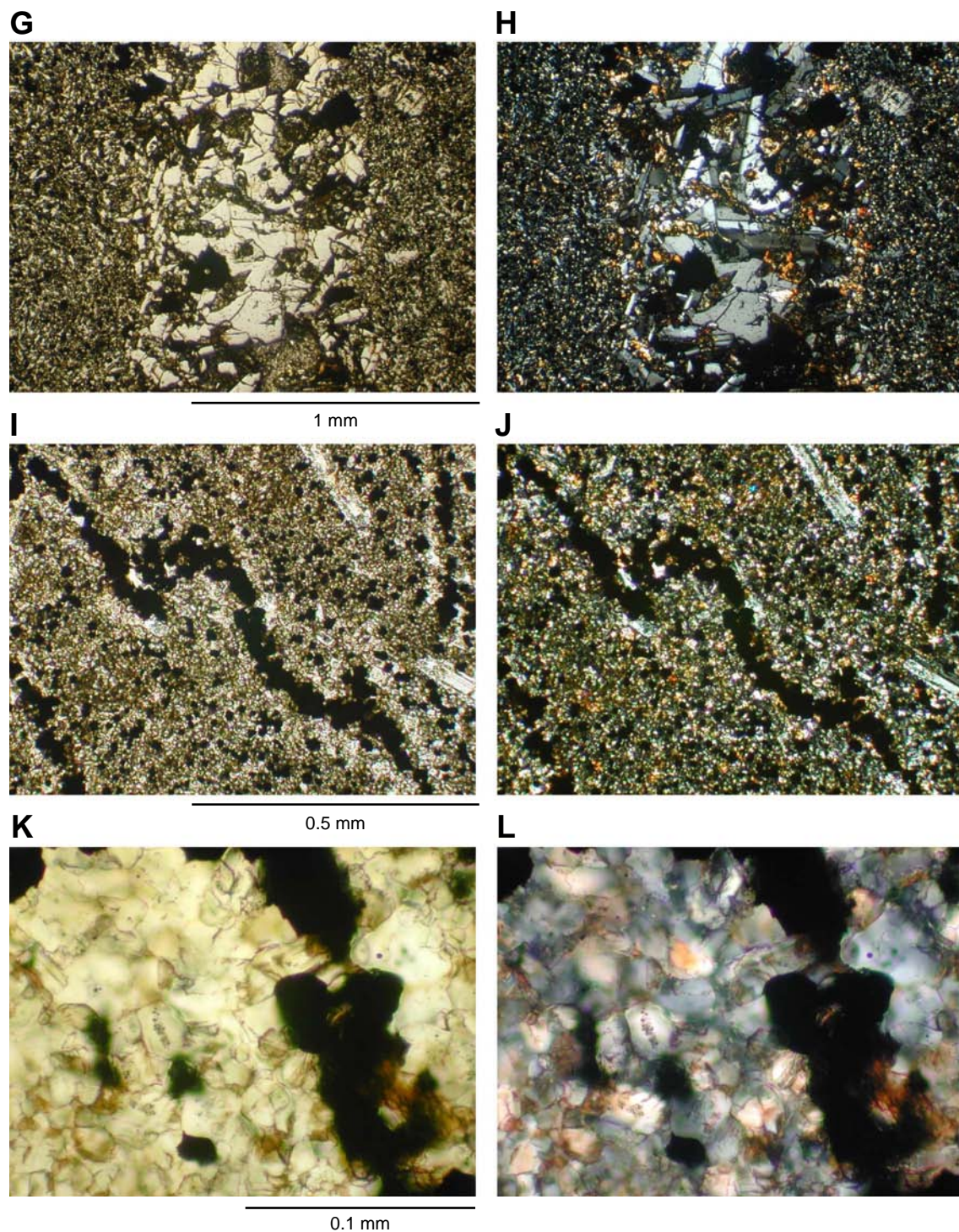


Figure F4 (continued). Selected photomicrographs of (M–R) Sample 206-1256C-11R-7, 96–100 cm, showing textural variations of the recrystallized base of Unit 1256C-18.

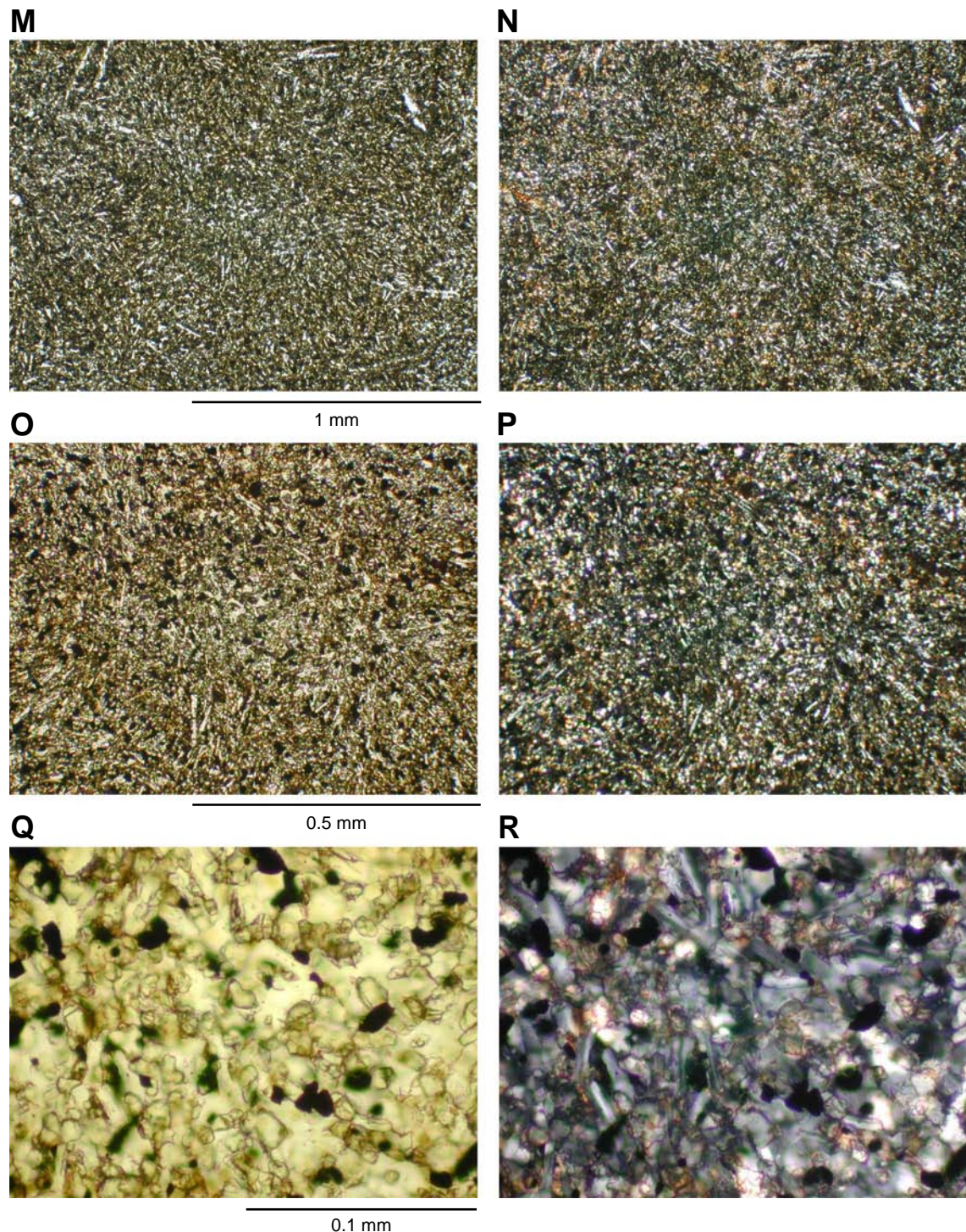


Figure F4 (continued). Selected photomicrographs of (S–X) Sample 206-1256C-11R-7, 130–133 cm, showing textural variations of the recrystallized base of Unit 1256C-18.

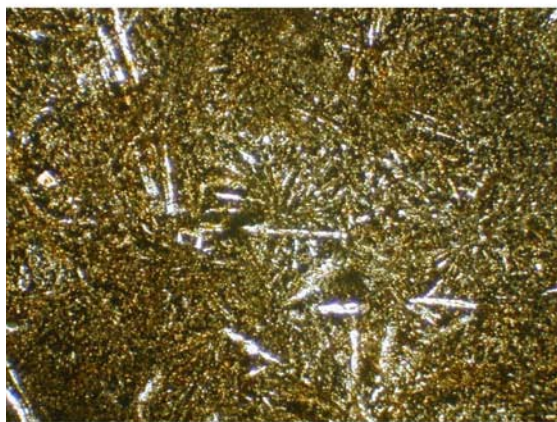
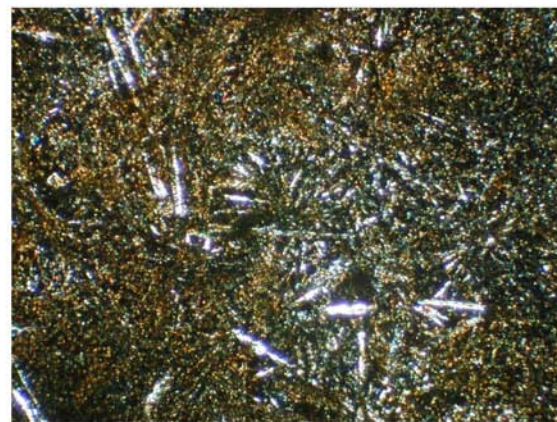
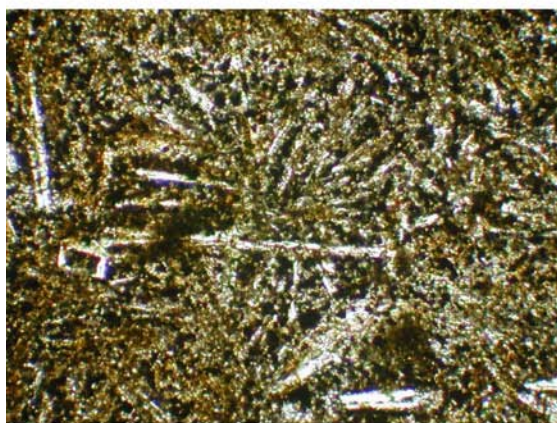
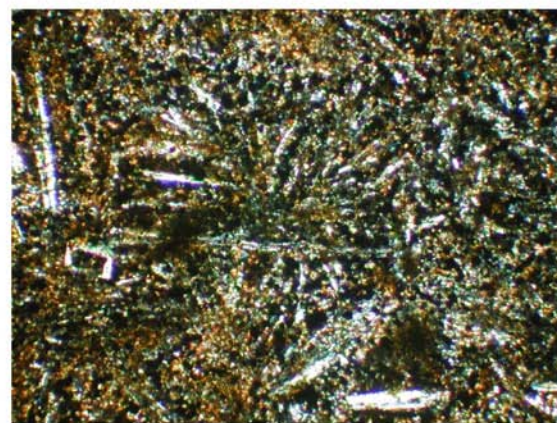
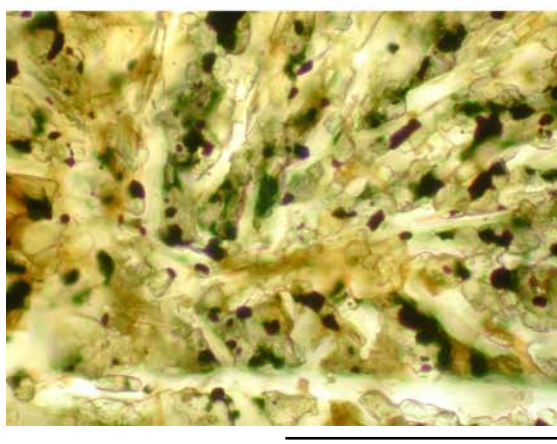
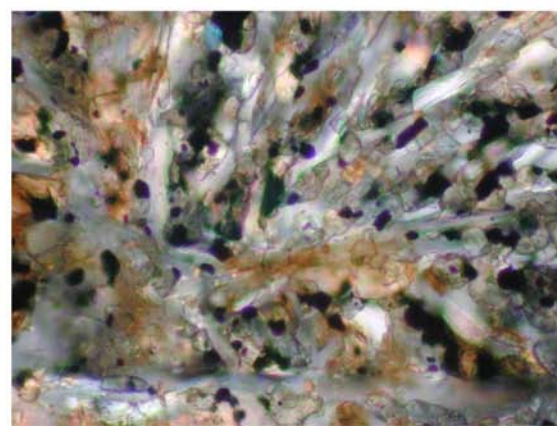
S**T****U****V****W****X**

Figure F5. SEM images of Sample 206-1256C-11R-7, 47–50 cm. A. Photomicrograph of a thin section showing locations of (B–G) SEM images. (Continued on next page.)

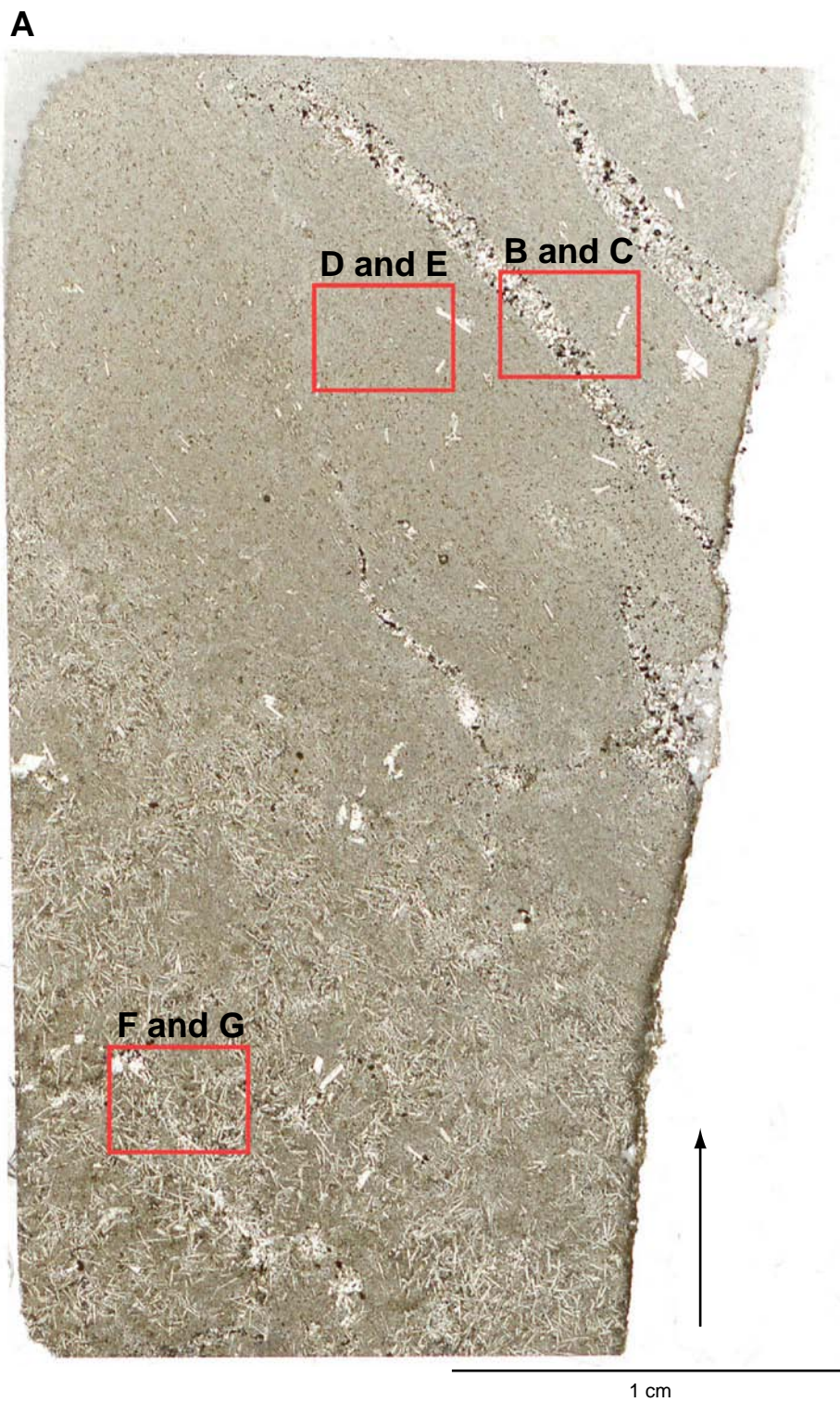


Figure F5 (continued). B, C. Coarse vein. D, E. Fine-grained groundmass. F, G. Coarse-grained plagioclase laths. Bright crystals are of Fe-Ti oxide, and gray and dark ones are of clinopyroxene and plagioclase, respectively.

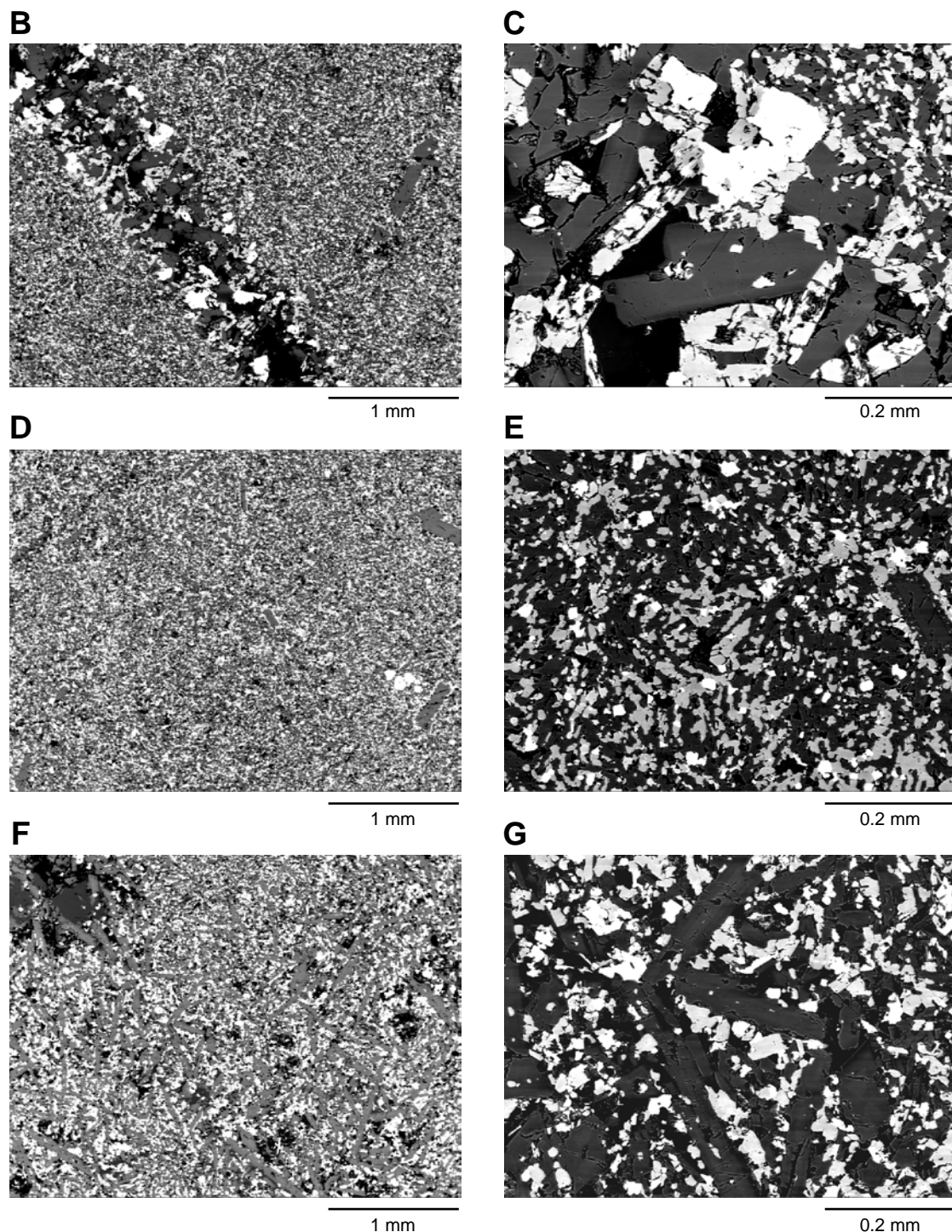


Figure F6. SEM images of Sample 206-1256C-11R-7, 76–79 cm. A. Photomicrograph of a thin section showing locations of (B–E) SEM images. (Continued on next page.)



Figure F6 (continued). B, C. Fine-grained groundmass. D, E. Coarse-grained plagioclase laths. Bright crystals are of Fe-Ti oxide, and gray and dark ones are of clinopyroxene and plagioclase, respectively.

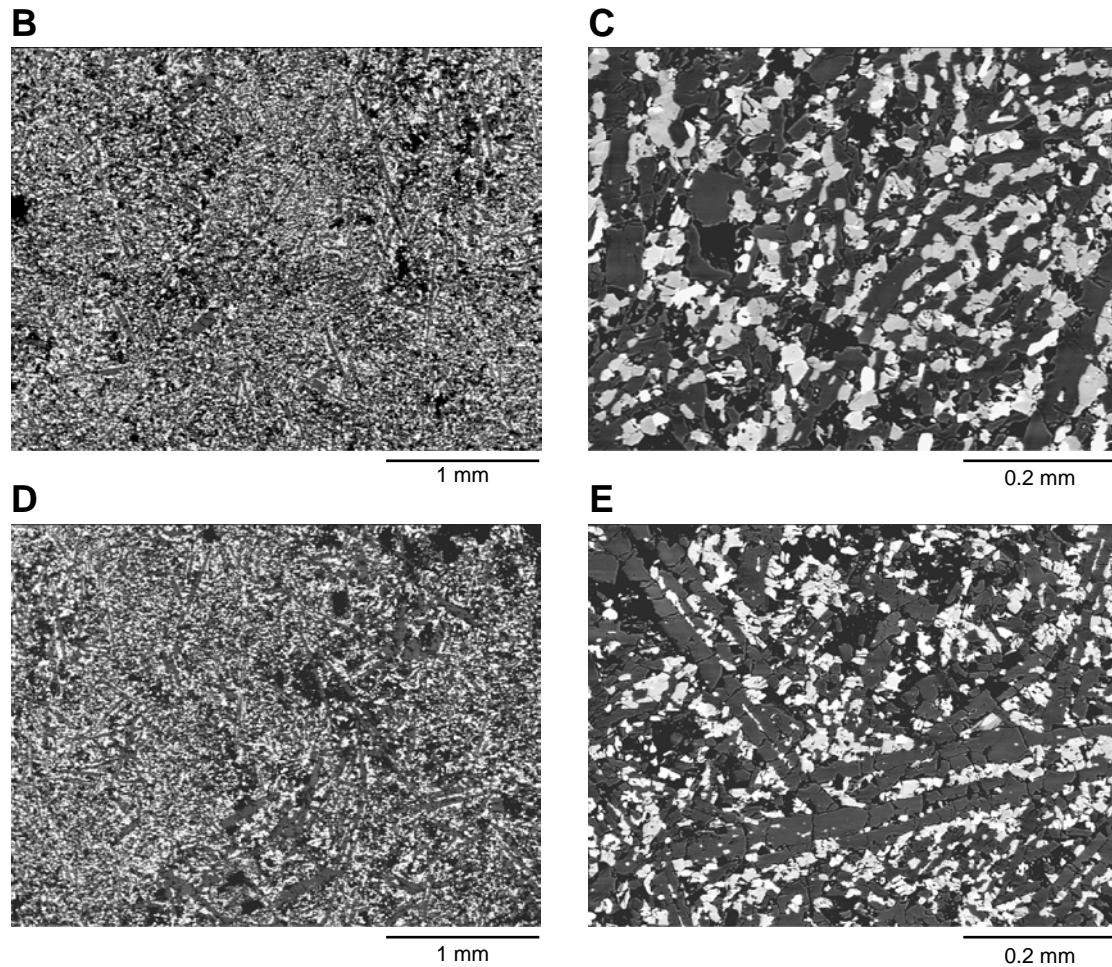


Figure F7. SEM images of Sample 206-1256C-11R-7, 96–100 cm. A. Photomicrograph of a thin section showing locations of (B–G) SEM images. (Continued on next page.)

A

Figure F7 (continued). B, C. Fine-grained groundmass. D, E. Coarse-grained plagioclase laths. F, G. Fine-grained groundmass. Bright crystals are of Fe-Ti oxide, and gray and dark ones are of clinopyroxene and plagioclase, respectively.

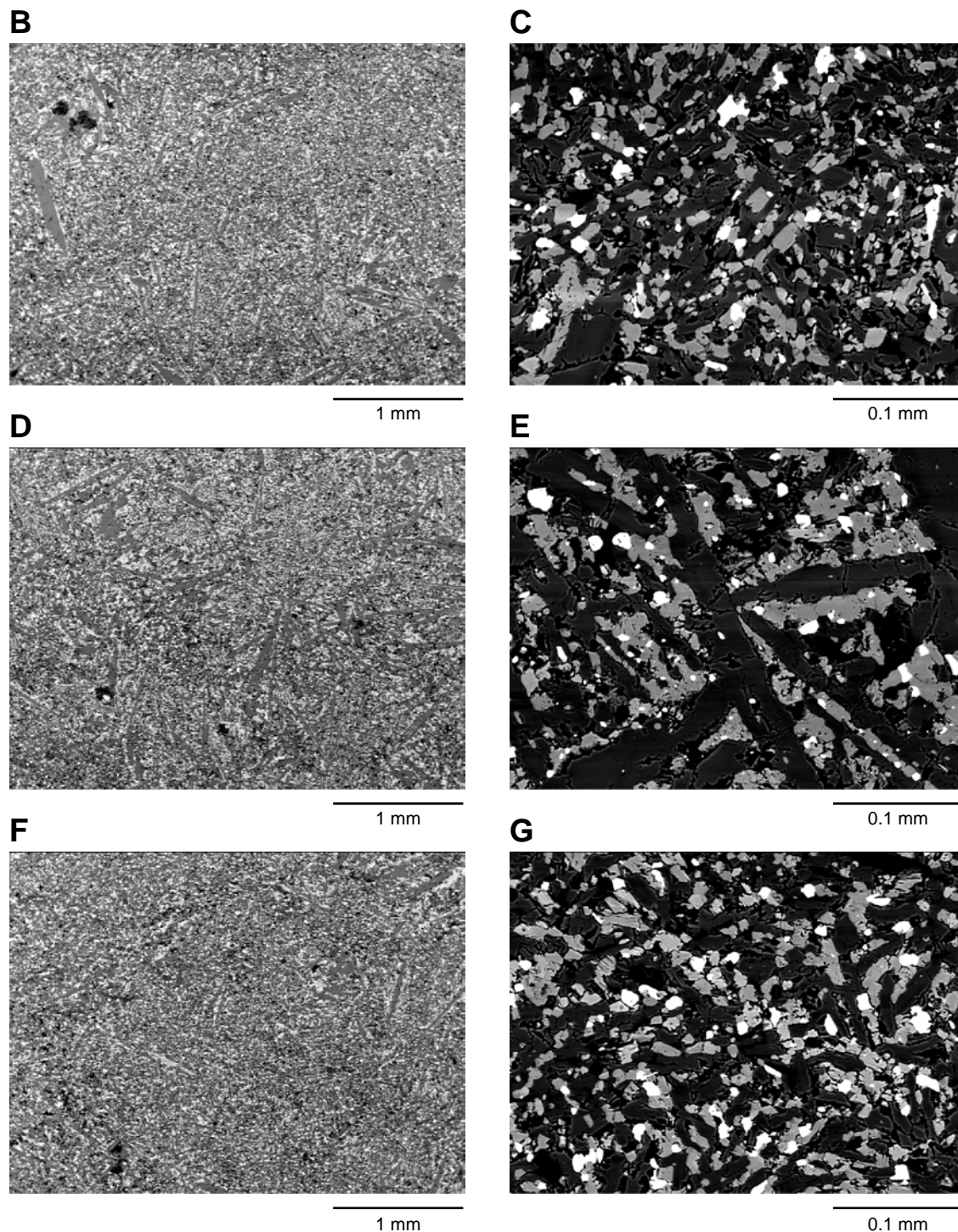


Figure F8. Grain size variations of the groundmass crystals in the base of the lava pond in Hole 1256C. (A) Clinopyroxene, (B) Magnetite, and (C) Plagioclase. Solid circles = average maximum length, open circles = average maximum width, squares = diameter of a circle with an equivalent area to the crystal, crosses = maximum width/length (W/L) ratio. (Continued on next page.)

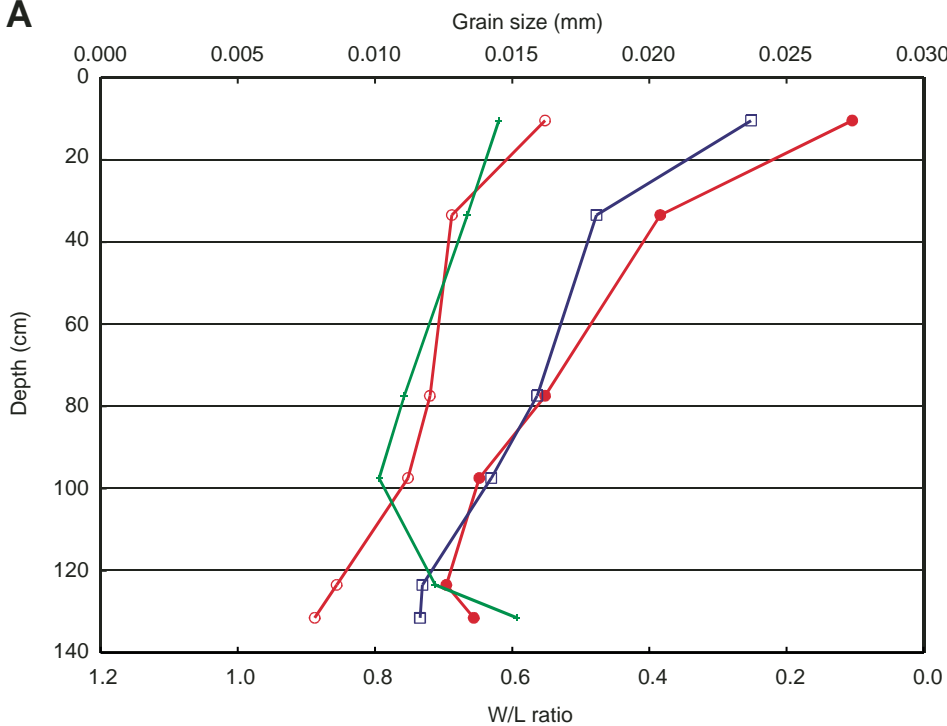
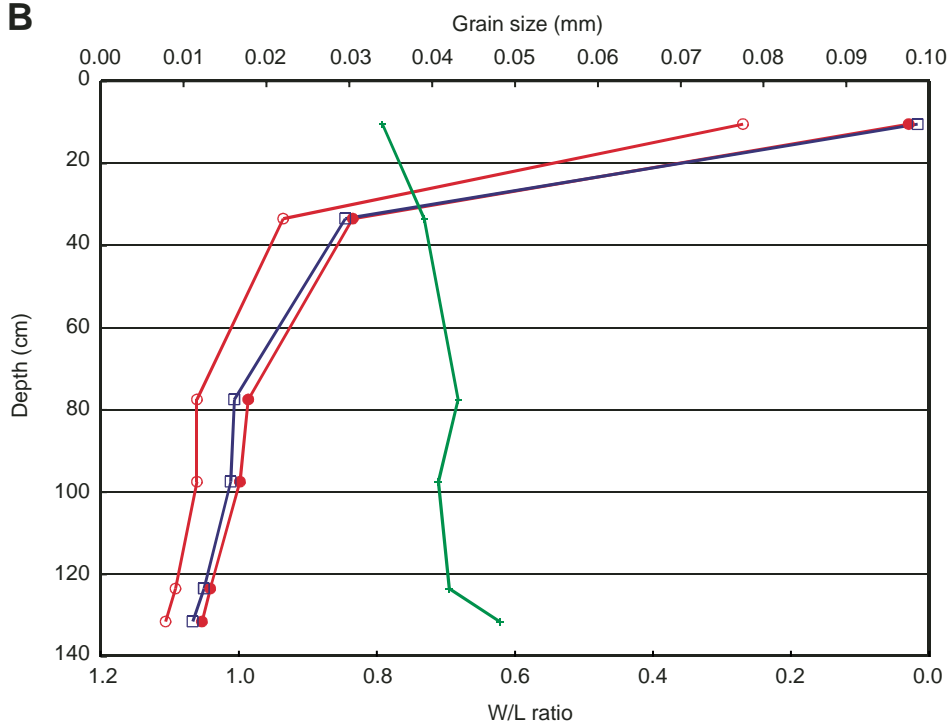
A**B**

Figure F8 (continued).

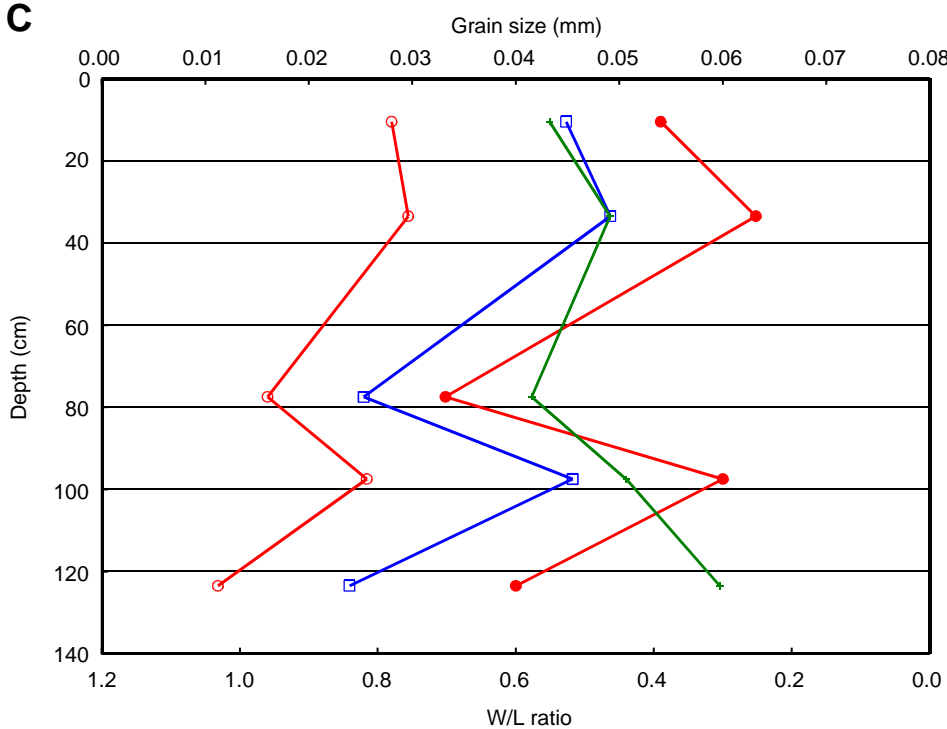
C

Figure F9. Mineral compositions of Samples 206-1256C-11R-7, 47–50 cm, 11R-7, 76–79 cm, and 11R-7, 96–100 cm. A. FeO wt% vs. An mol% of plagioclase. B. Clinopyroxene compositions plotted onto pyroxene quadrilateral. (Continued on next page.)

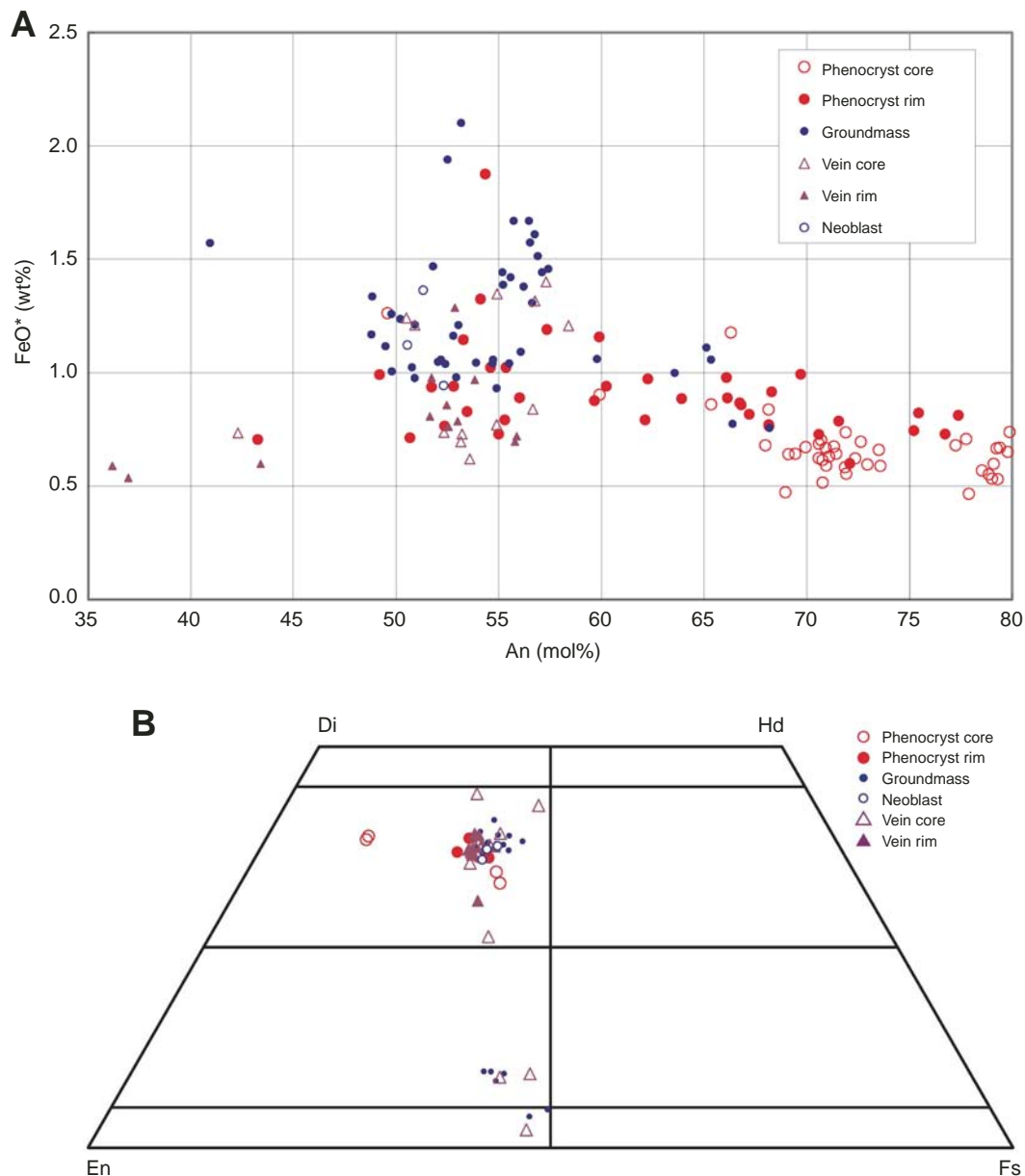


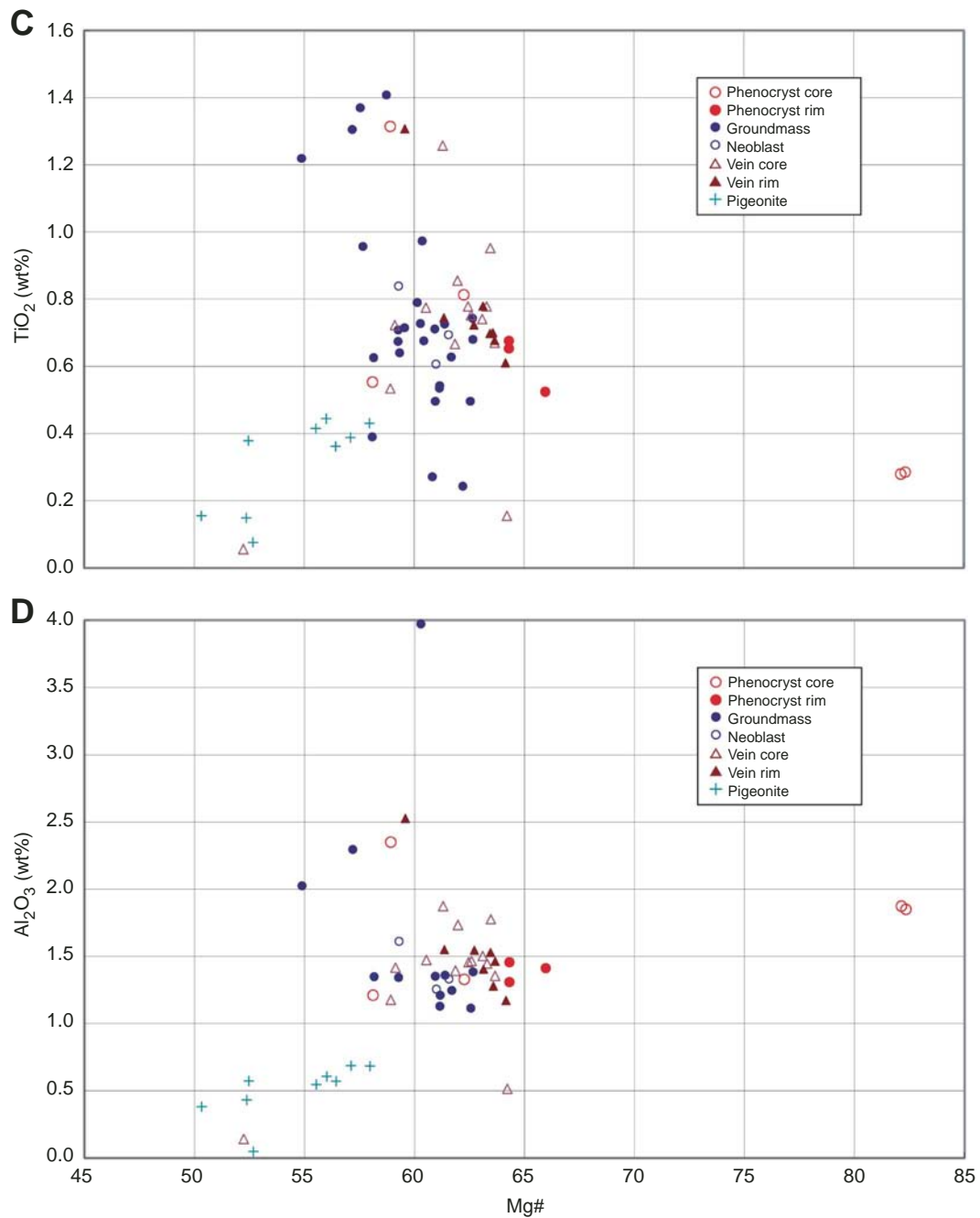
Figure F9 (continued). C. TiO_2 wt% vs. Mg# of clinopyroxene. D. Al_2O_3 wt% vs. Mg# of clinopyroxene.

Table T1. Average maximum grain sizes of Units 1256C-18 and 1256D-1. (See table notes. Continued on next page.)

Core, section, interval (cm)	Depth (mbsf)	Plagioclase					Clinopyroxene				
		Max	Min	Area	W/L	EQD	Max	Min	Area	W/L	EQD
206-1256C, Unit 18											
8R-6, 1–4	281.47	0.567	0.059	0.033	0.112	0.204	0.224	0.053	0.012	0.243	0.122
8R-6, 63–66	282.09	1.046	0.115	0.119	0.113	0.389	0.780	0.122	0.090	0.171	0.338
8R-6, 115–120	282.61	1.197	0.131	0.163	0.116	0.456	0.866	0.126	0.111	0.147	0.376
9R-1, 6–9	284.76	1.135	0.156	0.182	0.136	0.481	0.877	0.201	0.172	0.237	0.468
9R-1, 61–65	285.31	1.472	0.270	0.393	0.188	0.707	0.946	0.310	0.299	0.345	0.617
9R-2, 23–26	285.96	1.308	0.318	0.408	0.252	0.721	0.916	0.362	0.328	0.410	0.646
9R-2, 73–77	286.46	1.340	0.296	0.393	0.232	0.707	1.000	0.270	0.284	0.281	0.601
9R-2, 132–135	287.05	1.322	0.320	0.435	0.239	0.744	0.908	0.298	0.280	0.338	0.597
9R-3, 33–36	287.56	1.982	0.466	0.862	0.257	1.048	1.480	0.330	0.495	0.233	0.794
9R-3, 93–96	288.16	1.716	0.546	0.945	0.351	1.097	1.412	0.322	0.474	0.244	0.777
9R-4, 3–6	288.73	2.696	0.534	1.534	0.211	1.398	1.418	0.494	0.713	0.334	0.953
9R-4, 62–68	289.32	1.818	0.456	0.855	0.256	1.044	1.660	0.452	0.756	0.272	0.981
9R-4, 121–124	289.91	2.328	0.520	1.247	0.223	1.260	1.602	0.476	0.821	0.297	1.022
9R-5, 33–36	290.50	1.366	0.258	0.369	0.192	0.686	1.468	0.400	0.568	0.301	0.851
9R-5, 94–97	291.11	1.682	0.446	0.746	0.306	0.975	0.736	0.366	0.268	0.518	0.584
9R-6, 6–9	291.72	2.568	0.998	2.476	0.406	1.775	0.838	0.316	0.247	0.434	0.561
9R-6, 71–75	292.37	2.070	0.824	1.697	0.413	1.470	0.904	0.298	0.277	0.353	0.593
9R-6, 123–126	292.89	1.870	0.688	1.344	0.383	1.308	1.268	0.386	0.533	0.288	0.823
9R-7, 33–36	293.41	1.662	0.436	0.718	0.274	0.956	1.022	0.322	0.320	0.348	0.639
9R-7, 73–76	293.81	1.588	0.408	0.649	0.259	0.909	0.802	0.260	0.209	0.334	0.516
9R-7, 89–93	293.97	1.704	0.494	0.886	0.306	1.062	0.970	0.344	0.329	0.383	0.647
9R-7, 122–127	294.30	1.674	0.408	0.674	0.261	0.927	0.648	0.334	0.221	0.528	0.531
9R-8, 21–23	294.72	1.742	0.624	1.079	0.376	1.172	0.786	0.200	0.158	0.254	0.449
10R-1, 43–46	294.33	1.566	0.448	0.710	0.289	0.951	0.768	0.218	0.171	0.301	0.467
10R-1, 104–107	294.94	1.584	0.362	0.556	0.249	0.841	0.830	0.286	0.241	0.348	0.553
10R-2, 13–16	295.48	1.768	0.490	0.834	0.292	1.030	1.258	0.376	0.452	0.310	0.759
10R-2, 65–68	296.00	1.772	0.374	0.710	0.209	0.951	0.876	0.420	0.361	0.487	0.678
10R-2, 105–108	296.40	1.474	0.302	0.459	0.213	0.764	1.016	0.396	0.390	0.415	0.705
10R-3, 13–16	296.93	1.774	0.300	0.551	0.175	0.837	0.840	0.336	0.275	0.428	0.592
10R-3, 47–50	297.27	1.592	0.312	0.488	0.204	0.789	0.806	0.316	0.238	0.421	0.550
10R-3, 102–105	297.82	1.618	0.414	0.682	0.259	0.932	0.832	0.366	0.320	0.466	0.638
10R-4, 43–46	298.29	1.826	0.480	0.916	0.261	1.080	0.764	0.368	0.277	0.510	0.594
10R-4, 108–111	298.94	1.514	0.314	0.453	0.215	0.760	0.848	0.388	0.317	0.510	0.635
10R-5, 40–43	299.56	1.434	0.256	0.374	0.176	0.690	0.820	0.440	0.361	0.571	0.678
10R-5, 83–86	299.99	1.718	0.366	0.628	0.228	0.894	0.742	0.422	0.322	0.598	0.640
10R-6, 53–56	300.66	1.290	0.338	0.444	0.278	0.752	0.690	0.440	0.310	0.638	0.628
10R-6, 78–79	300.91	1.420	0.432	0.621	0.296	0.889	0.754	0.374	0.290	0.531	0.607
11R-1, 55–58	303.85	1.774	0.340	0.637	0.195	0.900	0.848	0.430	0.378	0.524	0.693
11R-1, 113–116	304.43	1.370	0.248	0.362	0.183	0.679	0.742	0.428	0.330	0.569	0.648
11R-2, 23–26	305.02	1.400	0.350	0.493	0.240	0.792	0.928	0.516	0.497	0.574	0.796
11R-2, 79–82	305.58	1.364	0.276	0.369	0.208	0.685	0.858	0.430	0.366	0.554	0.683
11R-2, 140–143	306.19	1.524	0.356	0.526	0.251	0.818	0.828	0.428	0.354	0.536	0.671
11R-3, 67–71	306.92	1.364	0.276	0.369	0.208	0.685	0.914	0.592	0.579	0.663	0.859
11R-3, 116–119	307.41	1.440	0.314	0.468	0.205	0.772	0.816	0.406	0.337	0.519	0.655
11R-4, 25–28	308.00	1.562	0.260	0.410	0.169	0.723	0.700	0.372	0.278	0.554	0.595
11R-4, 84–87	308.59	1.778	0.272	0.482	0.163	0.783	0.862	0.434	0.387	0.527	0.702
11R-5, 4–7	309.26	1.804	0.288	0.528	0.168	0.820	1.084	0.528	0.603	0.520	0.876
11R-5, 63–66	309.85	1.756	0.356	0.630	0.212	0.896	1.100	0.602	0.646	0.593	0.907
11R-5, 120–123	310.42	1.534	0.214	0.327	0.141	0.645	1.056	0.508	0.523	0.505	0.816
11R-6, 47–50	311.15	1.336	0.260	0.352	0.201	0.669	0.732	0.316	0.226	0.472	0.537
11R-6, 99–102	311.67	1.512	0.282	0.449	0.191	0.756	0.811	0.297	0.234	0.385	0.546
11R-6, 124–127	311.92	0.795	0.103	0.082	0.131	0.322	0.443	0.133	0.058	0.301	0.272
206-1256D, Unit 1											
2R-1, 33–36	276.45	1.351	0.195	0.272	0.139	0.588	0.808	0.282	0.233	0.323	0.544
2R-1, 53–56	276.65	1.312	0.222	0.288	0.177	0.606					
2R-1, 85–87	276.96	1.236	0.206	0.247	0.172	0.561					
2R-1, 87–91	276.99	1.154	0.180	0.211	0.156	0.518	1.100	0.240	0.272	0.224	0.589
3R-1, 68–71	278.80	1.348	0.241	0.318	0.181	0.637	1.162	0.328	0.386	0.298	0.701
3R-2, 53–56	279.96	1.462	0.291	0.428	0.004	0.738	1.349	0.353	0.469	0.006	0.773
3R-3, 61–64	281.15	2.222	0.462	1.078	0.219	1.172	1.840	0.370	0.717	0.209	0.956
3R-3, 85–89	281.39	3.010	0.498	1.535	0.189	1.398					
4R-1, 10–13	285.22	1.830	0.676	1.273	0.357	1.273	1.556	0.338	0.579	0.208	0.859
4R-1, 93–96	286.05	2.122	0.612	1.269	0.295	1.271					
4R-2, 58–62	287.09	2.200	0.708	1.772	0.322	1.502	1.264	0.314	0.386	0.267	0.701
4R-3, 76–78	288.47	2.088	0.552	1.184	0.267	1.228					
4R-3, 77–81	288.49	2.020	0.602	1.222	0.297	1.247	1.296	0.368	0.478	0.309	0.780

Table T1 (continued).

Core, section, interval (cm)	Depth (mbsf)	Plagioclase					Clinopyroxene				
		Max	Min	Area	W/L	EQD	Max	Min	Area	W/L	EQD
4R-4, 74–76	289.81	1.746	0.488	0.859	0.273	1.046					
4R-4, 75–80	289.84	1.464	0.406	0.577	0.302	0.857	1.194	0.546	0.651	0.463	0.910
4R-4, 116–119	290.24	1.684	0.452	0.757	0.271	0.982	1.228	0.368	0.439	0.326	0.748
5R-3, 3–6	292.82	1.530	0.344	0.516	0.240	0.811	0.830	0.342	0.266	0.428	0.582
5R-4, 5–8	293.87	1.554	0.350	0.519	0.242	0.813					
5R-4, 7–11	293.89	1.562	0.404	0.609	0.272	0.881	0.684	0.338	0.219	0.944	0.528
6R-2, 49–52	296.41	1.664	0.404	0.676	0.256	0.928	0.962	0.380	0.360	0.411	0.677
6R-4, 29–32	298.75	1.390	0.282	0.390	0.202	0.704	0.666	0.258	0.180	0.415	0.479
6R-5, 102–106	300.75	1.426	0.340	0.532	0.235	0.823	0.658	0.230	0.147	0.358	0.433
6R-5, 107–109	300.79	1.536	0.274	0.415	0.182	0.727					
6R-6, 51–54	301.55	1.486	0.314	0.484	0.222	0.785	0.692	0.231	0.161	0.352	0.453
6R-7, 83–86	303.39	1.560	0.308	0.463	0.201	0.767					
7R-2, 66–69	306.05	1.638	0.501	0.822	0.314	1.023	0.808	0.272	0.218	0.373	0.527
7R-3, 86–88	307.55	1.914	0.394	0.742	0.221	0.972					
7R-6, 91–94	311.67	1.802	0.409	0.755	0.242	0.981	0.640	0.294	0.200	0.459	0.505
8R-1, 62–66	313.94	1.691	0.348	0.611	0.206	0.882	0.682	0.346	0.236	0.504	0.548
8R-2, 63–67	315.38	1.674	0.320	0.541	0.211	0.830	0.748	0.308	0.223	0.430	0.532
8R-2, 67–69	315.41	1.600	0.330	0.533	0.211	0.824					
8R-6, 46–49	319.59	1.820	0.348	0.611	0.198	0.882					
8R-7, 96–99	321.18	1.350	0.266	0.351	0.203	0.668	0.788	0.348	0.262	0.518	0.578
9R-1, 3–7	322.85	1.286	0.388	0.494	0.297	0.793	0.702	0.316	0.211	0.508	0.518
9R-2, 7–9	324.07	1.634	0.260	0.447	0.164	0.755					
9R-5, 62–65	328.46	1.394	0.276	0.378	0.199	0.693					
10R-1, 4–7	327.46	1.268	0.338	0.409	0.277	0.721	0.754	0.354	0.265	0.486	0.581
10R-1, 110–113	328.52	1.470	0.250	0.354	0.174	0.671					
10R-2, 28–30	329.18	1.642	0.248	0.415	0.149	0.727					
11R-1, 8–11	332.00	1.616	0.322	0.27347	0.004	5.901	0.798	0.380	15.138	0.010	4.390
11R-3, 33–37	334.89	1.267	0.360	0.23571	0.005	5.478	0.750	0.378	0.279	0.541	0.596
11R-3, 39–42	334.95	1.388	0.248	0.360	0.180	0.677					
12R-1, 5–8	341.27	1.360	0.344	0.464	0.270	0.769	0.754	0.386	0.292	0.539	0.610
12R-4, 59–62	346.03	1.264	0.328	0.426	0.256	0.736	0.840	0.410	0.355	0.506	0.672
12R-6, 39–42	348.24	1.126	0.174	0.192	0.157	0.495	0.552	0.210	0.118	0.401	0.387
12R-7, 83–86	349.59	2.048	0.210	0.428	0.106	0.739					
12R-7, 85–89	349.98	0.908	0.130	0.111	0.147	0.376	0.532	0.220	0.114	0.494	0.382

Notes: W/L = width/length ratio. EQD = diameter of a circle with equivalent area to a crystal.

Table T2. Average maximum grain sizes of recrystallized base of Unit 1256C-18.

Core, section, interval (cm)	Depth (mbsf)	Plagioclase					Clinopyroxene					Magnetite				
		Max	Min	Area	W/L	EQD	Max	Min	Area	W/L	EQD	Max	Min	Area	W/L	EQD
206-1256C-																
11R-7, 9–12	312.13	0.02700	0.01400	0.00040	0.55105	0.022	0.027	0.016	0.00044	0.620	0.024	0.0975	0.0775	0.00763	0.7923	0.099
11R-7, 32–35	312.36	0.03160	0.01480	0.00047	0.46358	0.025	0.020	0.013	0.00026	0.666	0.018	0.0304	0.0220	0.00068	0.7318	0.030
11R-7, 76–79	312.80	0.01660	0.00800	0.00013	0.57706	0.013	0.016	0.012	0.00020	0.758	0.016	0.0178	0.0116	0.00020	0.6825	0.016
11R-7, 96–99	313.00	0.03000	0.01280	0.00041	0.44008	0.023	0.014	0.011	0.00016	0.794	0.014	0.0168	0.0116	0.00019	0.7112	0.016
11R-7, 122–125	313.26	0.02000	0.00560	0.00011	0.30434	0.012	0.013	0.009	0.00011	0.712	0.012	0.0132	0.0090	0.00012	0.6952	0.012
11R-7, 130–133	313.34						0.014	0.008	0.00011	0.593	0.012	0.0122	0.0078	0.00010	0.6221	0.011

Notes: W/L = width/length ratio. EQD = diameter of a circle with equivalent area to a crystal.

Table T3. Mineral compositions from Hole 1256C, ODP206, Guatemala Basin. (See table notes. Continued on next three pages.)

Analysis number	Mode	Normalized mineral percentages									Major element oxide (wt%)													
		An	Ab	Or	Wo	En	Fs	YAl	YCr	YFe	Mg#	SiO ₂	TiO ₂	Al ₂ O ₃	FeO*	MnO	MgO	CaO	Na ₂ O	K ₂ O	Cr ₂ O ₃	NiO	V ₂ O ₃	Total
A: 206-1256C-11R-7, 47–50 cm																								
<i>Plagioclase</i>																								
050424-128	Pod-1	VC	58.40	41.42	0.19						19.34	53.22	0.03	27.62	1.24	0.00	0.17	11.93	4.68	0.03	0.00	0.00	0.00	98.92
050424-129	Pod-1	VR	43.40	55.50	1.10						9.94	56.11	0.00	26.09	0.60	0.00	0.04	8.91	6.30	0.19	0.00	0.00	0.00	98.24
050424-130	Pod-1	VC	57.30	42.39	0.31						13.42	53.46	0.07	28.17	1.21	0.00	0.11	11.75	4.80	0.05	0.02	0.00	0.00	99.63
050424-131	Pod-1	VR	52.46	47.03	0.50						12.39	55.83	0.05	28.43	0.86	0.00	0.07	10.93	5.41	0.09	0.00	0.00	0.00	101.66
050424-132	Pod-1	VC	54.91	44.65	0.44						15.12	55.11	0.07	27.94	1.40	0.00	0.14	11.18	5.02	0.08	0.00	0.00	0.00	100.94
050424-133	Pod-1	VR	36.17	62.10	1.73						2.94	60.05	0.00	26.34	0.59	0.00	0.01	7.73	7.33	0.31	0.00	0.00	0.00	102.36
050424-136	Pod-1	VC	56.75	43.03	0.21						17.65	53.02	0.07	28.04	1.35	0.00	0.16	11.65	4.88	0.04	0.00	0.00	0.00	99.20
050424-137	Pod-1	VR	53.83	45.64	0.54						14.34	54.52	0.07	28.71	0.97	0.00	0.09	11.26	5.28	0.09	0.00	0.00	0.00	100.99
050424-138	Pod-1	VC	56.66	42.96	0.39						16.22	53.82	0.05	28.43	1.32	0.00	0.14	11.84	4.96	0.07	0.00	0.00	0.00	100.63
050424-139	Pod-1	VR	52.55	46.49	0.96						11.95	55.28	0.03	28.12	0.76	0.00	0.06	11.00	5.38	0.17	0.01	0.00	0.01	100.81
050424-146	Pod-1	VC	50.91	48.61	0.49						11.79	55.53	0.03	28.67	0.84	0.00	0.06	10.74	5.67	0.09	0.00	0.00	0.00	101.63
050424-147	Pod-1	VR	51.72	47.64	0.63						10.59	54.95	0.04	28.57	0.98	0.00	0.07	10.79	5.49	0.11	0.00	0.00	0.00	100.98
050424-155	Pod-1	VC	42.30	56.22	1.48						3.69	57.02	0.55	26.81	1.21	0.00	0.03	8.88	6.52	0.26	0.00	0.00	0.00	101.27
050424-158	Clot-1	PC	70.77	29.17	0.05						42.05	51.42	0.00	31.16	0.52	0.00	0.21	14.77	3.36	0.01	0.02	0.00	0.00	101.46
050424-159	Clot-1	PR	68.16	31.70	0.14						16.37	52.40	0.02	31.58	0.77	0.00	0.08	14.17	3.64	0.02	0.00	0.00	0.00	102.69
050424-160	Clot-1	PC	71.92	27.90	0.18						40.28	51.10	0.00	31.84	0.56	0.00	0.21	14.66	3.14	0.03	0.00	0.00	0.00	101.54
050424-161	Clot-1	PR	55.35	43.86	0.79						26.04	54.65	0.02	28.68	1.02	0.00	0.20	11.35	4.97	0.14	0.00	0.00	0.00	101.03
050424-162	Clot-1	PC	68.96	30.96	0.08						43.95	51.36	0.02	30.72	0.47	0.00	0.21	14.11	3.50	0.01	0.00	0.00	0.00	100.40
050424-163	Clot-1	PR	50.67	48.82	0.51						16.50	55.80	0.02	28.26	0.71	0.00	0.08	10.66	5.68	0.09	0.00	0.00	0.00	101.30
050424-164	Clot-1	PC	59.91	39.85	0.24						23.66	53.58	0.03	29.42	0.90	0.00	0.16	12.55	4.61	0.04	0.00	0.00	0.00	101.30
050424-165	Clot-1	PR	53.46	45.96	0.59						15.30	54.00	0.08	28.73	0.83	0.00	0.08	11.09	5.27	0.10	0.00	0.00	0.00	100.19
050424-178	Vein-1	VC	54.89	44.83	0.27						18.91	54.58	0.05	27.83	0.73	0.00	0.10	11.10	5.01	0.05	0.00	0.00	0.00	99.44
050424-179	Vein-1	VR	5.56	93.01	1.43						0.00	69.97	0.00	20.89	0.28	0.00	0.00	1.17	10.77	0.25	0.00	0.00	0.00	103.32
050424-180	Vein-1	VC	53.58	46.12	0.30						17.54	54.88	0.04	28.33	0.77	0.00	0.09	11.20	5.33	0.05	0.00	0.00	0.00	100.70
050424-181	Vein-1	VR	52.99	46.57	0.44						18.47	55.42	0.05	28.60	0.79	0.00	0.10	10.95	5.32	0.08	0.00	0.00	0.00	101.32
050424-182	Vein-1	VC	53.14	46.50	0.36						20.92	55.98	0.06	28.18	0.62	0.00	0.09	11.10	5.37	0.06	0.00	0.00	0.00	101.47
050424-183	Vein-1	VR	55.87	43.85	0.28						14.05	54.81	0.00	28.58	0.72	0.00	0.07	11.70	5.07	0.05	0.00	0.00	0.00	100.99
050424-184	Vein-1	VC	52.33	47.36	0.31						14.09	56.79	0.06	28.02	0.70	0.00	0.06	10.76	5.38	0.05	0.00	0.00	0.00	101.83
050424-185	Vein-1	VR	51.64	47.96	0.40						13.87	56.59	0.06	28.97	0.81	0.00	0.07	11.09	5.69	0.07	0.00	0.00	0.00	103.34
050424-188	Vein-1	VC	53.21	46.47	0.32						19.01	55.33	0.04	27.89	0.74	0.00	0.10	11.17	5.39	0.06	0.00	0.00	0.00	100.71
050424-189	Vein-1	VR	36.95	60.90	2.15						5.04	56.92	0.00	24.76	0.54	0.00	0.02	7.56	6.89	0.37	0.00	0.00	0.00	97.05
050424-190	Vein-1	VC	53.98	45.73	0.29						20.26	54.77	0.07	27.66	0.73	0.00	0.10	11.23	5.26	0.05	0.00	0.00	0.00	99.87
050424-191	Vein-1	VR	55.79	43.86	0.36						17.34	53.32	0.14	28.72	0.70	0.00	0.08	11.67	5.07	0.06	0.00	0.00	0.00	99.76
<i>Clinopyroxene</i>																								
050424-140	Pod-1	VC				42.67	29.95	27.38			52.24	52.74	0.06	0.14	16.10	0.34	9.88	19.58	0.79	0.01	0.06	0.00	0.14	99.85
050424-141	Pod-1	VC				44.10	35.90	20.00			64.22	53.49	0.16	0.52	12.04	0.30	12.12	20.72	0.39	0.00	0.00	0.04	0.04	99.78
050424-142	Pod-1	VC				37.69	37.72	24.59			60.54	51.00	0.78	1.47	14.53	0.36	12.50	17.38	0.24	0.01	0.01	0.00	0.07	98.34
050424-143	Pod-1	VC				37.64	38.57	23.79			61.85	51.79	0.67	1.39	14.27	0.31	12.97	17.62	0.21	0.01	0.00	0.03	0.10	99.36
050424-144	Pod-1	VC				37.99	38.73	23.29			62.45	51.51	0.78	1.46	14.02	0.36	13.08	17.85	0.25	0.01	0.00	0.00	0.08	99.40
050424-145	Pod-1	VC				37.87	38.88	23.24			62.59	50.74	0.75	1.47	13.84	0.35	12.99	17.60	0.27	0.01	0.00	0.00	0.06	98.05
050424-148	Pod-1	VC				36.39	38.99	24.62			61.30	49.39	1.26	1.87	14.74	0.35	13.09	17.00	0.23	0.01	0.01	0.01	0.08	98.05
050424-149	Pod-1	VR				36.56	40.05	23.39			63.14	50.52	0.78	1.40	14.23	0.28	13.67	17.36	0.26	0.01	0.00	0.00	0.07	98.59
050424-150	Pod-1	VC				37.64	38.64	23.71			61.97	49.75	0.86	1.73	14.16	0.35	12.94	17.54	0.37	0.03	0.00	0.00	0.08	97.80
050424-151	Pod-1	VR				37.51	37.23	25.26			59.58	49.25	1.31	2.53	14.78	0.40	12.22	17.13	0.34	0.03	0.02	0.00	0.10	98.09
050424-172	Clot-1	PC				36.31	39.65	24.04			62.26	51.64	0.81	1.33	14.55	0.32	13.46	17.15	0.29	0.02	0.00	0.00	0.07	99.62
050424-173	Clot-1	PC				34.36	38.67	26.97			58.92	49.44	1.31	2.35	16.01	0.33	12.88	15.92	0.24	0.02	0.00	0.00	0.11	

Table T3 (continued).

Analysis number	Mode	Normalized mineral percentages									Major element oxide (wt%)													
		An	Ab	Or	Wo	En	Fs	YAl	YCr	YFe	Mg#	SiO ₂	TiO ₂	Al ₂ O ₃	FeO*	MnO	MgO	CaO	Na ₂ O	K ₂ O	Cr ₂ O ₃	NiO	V ₂ O ₃	Total
050424-171	Clot-1	GC			9.22	50.41	40.37				55.53	51.82	0.42	0.55	24.16	0.68	16.92	4.31	0.09	0.02	0.01	0.00	0.06	99.03
050424-174	Clot-1	GC			9.48	51.69	38.83				57.11	51.07	0.39	0.69	23.62	0.58	17.64	4.50	0.19	0.00	0.00	0.01	0.06	98.74
050424-175	Clot-1	GR			9.49	52.46	38.04				57.97	50.39	0.43	0.68	22.98	0.58	17.78	4.48	0.06	0.01	0.00	0.00	0.03	97.42
050424-192	Vein-1	VC			36.58	40.14	23.28				63.30	49.03	0.78	1.45	14.05	0.46	13.60	17.24	0.25	0.00	0.00	0.00	0.07	96.92
050424-193	Vein-1	VR			37.10	40.35	22.55				64.16	50.09	0.61	1.17	13.60	0.38	13.65	17.47	0.23	0.01	0.00	0.00	0.05	97.27
050424-194	Vein-1	VC			35.47	40.95	23.57				63.47	49.62	0.95	1.78	14.22	0.29	13.85	16.70	0.21	0.01	0.00	0.00	0.06	97.68
050424-195	Vein-1	VR			37.06	40.01	22.92				63.58	51.03	0.70	1.28	13.96	0.43	13.67	17.62	0.25	0.01	0.01	0.00	0.04	99.01
050424-196	Vein-1	VC			2.22	51.50	46.28				52.68	50.88	0.08	0.05	28.00	0.74	17.48	1.05	0.02	0.01	0.00	0.00	0.06	98.36
050424-197	Vein-1	VR			30.74	42.49	26.77				61.36	50.96	0.75	1.55	16.17	0.38	14.40	14.50	0.18	0.00	0.01	0.00	0.08	98.97
050424-198	Vein-1	VC			37.59	39.38	23.04				63.10	51.50	0.74	1.50	13.83	0.38	13.26	17.61	0.23	0.01	0.00	0.00	0.05	99.13
050424-199	Vein-1	VR			36.80	40.23	22.97				63.66	51.65	0.68	1.46	13.87	0.36	13.63	17.35	0.23	0.01	0.00	0.00	0.07	99.29
050424-200	Vein-1	VC			39.17	35.84	24.99				58.92	50.49	0.53	1.18	15.01	0.35	12.07	18.36	0.27	0.01	0.00	0.00	0.04	98.31
050424-201	Vein-1	VR			38.94	38.29	22.76				62.72	51.36	0.72	1.55	13.79	0.41	13.01	18.41	0.22	0.01	0.00	0.00	0.04	99.52
050424-202	Vein-1	VC			26.30	43.57	30.12				59.13	51.15	0.72	1.42	18.00	0.48	14.61	12.27	0.18	0.01	0.00	0.00	0.05	98.88
050424-203	Vein-1	VR			39.14	38.62	22.24				63.46	51.85	0.70	1.53	13.38	0.41	13.03	18.37	0.24	0.00	0.02	0.00	0.06	99.59
050424-204	Vein-1	VC			37.50	39.78	22.71				63.66	51.55	0.67	1.36	13.66	0.34	13.43	17.61	0.21	0.02	0.00	0.00	0.07	98.90
<i>Ilmenite</i>																								
050424-152	Pod-1	VC									2.33	0.00	47.93	0.04	48.86	0.55	0.65	0.16	0.03	0.06	0.01	0.08	0.05	
050424-154	Pod-1	VC									3.69	0.00	48.47	0.06	47.57	0.50	1.02	0.11	0.03	0.04	0.01	0.12	0.05	
050424-156	Pod-1	VC									2.27	0.01	48.20	0.05	48.59	0.51	0.63	0.19	0.04	0.05	0.00	0.06	0.13	
050424-169	Clot-1	VC									4.09	0.02	47.90	0.09	47.14	0.45	1.13	0.11	0.02	0.04	0.05	0.12	0.16	
050424-170	Clot-1	VC									2.39	0.02	48.35	0.07	48.61	0.48	0.67	0.07	0.07	0.04	0.05	0.09	0.10	
<i>Magnetite</i>																								
050424-153	Pod-1	VC			2.19	0.37	97.44	0.65	0.03	12.11	0.76	53.03	29.26	0.29	0.28	0.14	0.02	0.06	0.19	0.12	1.12			
050424-157	Pod-1	VC			2.14	0.53	97.33	0.62	0.09	9.40	0.77	55.06	28.97	0.25	0.27	0.25	0.03	0.05	0.29	0.09	1.10			
B: 206-1256C-11R-7, 76-79 cm																								
<i>Plagioclase</i>																								
050424-057	Clot-1	PC	79.31	20.64	0.05						39.07	47.72	0.01	32.20	0.53	0.00	0.19	16.09	2.31	0.01	0.00	0.00	0.00	99.06
050424-058	Clot-1	PR	62.26	37.50	0.25						21.33	52.48	0.02	28.64	0.97	0.00	0.15	12.85	4.28	0.04	0.00	0.00	0.00	99.43
050424-059	Clot-1	PC	78.53	21.44	0.03						25.98	47.92	0.02	31.08	0.57	0.00	0.11	16.00	2.41	0.01	0.00	0.00	0.00	98.11
050424-060	Clot-1	PR	68.15	31.62	0.23						28.34	51.32	0.02	30.18	0.77	0.00	0.17	13.94	3.57	0.04	0.00	0.00	0.00	100.00
050424-061	Clot-1	PC	70.59	29.23	0.18						31.35	50.84	0.00	30.34	0.69	0.00	0.18	14.50	3.32	0.03	0.01	0.00	0.01	99.90
050424-062	Clot-1	PR	63.91	35.63	0.46						15.19	52.50	0.04	29.65	0.89	0.00	0.09	13.12	4.04	0.08	0.00	0.00	0.00	100.39
050424-063	Clot-1	PC	71.43	28.38	0.18						26.79	50.38	0.00	30.96	0.64	0.00	0.13	14.50	3.18	0.03	0.00	0.00	0.00	99.82
050424-064	Clot-1	PR	52.80	46.46	0.74						15.53	55.70	0.03	27.96	0.94	0.00	0.10	11.10	5.40	0.13	0.01	0.00	0.00	101.37
050424-065	Clot-1	PC	79.79	20.14	0.06						23.95	48.00	0.02	32.38	0.65	0.00	0.12	16.39	2.29	0.01	0.00	0.00	0.00	99.84
050424-066	Clot-1	PR	57.34	42.26	0.40						18.44	53.92	0.00	28.18	1.19	0.00	0.15	11.87	4.83	0.07	0.00	0.00	0.01	100.21
050424-070	Clot-1	PC	79.41	20.50	0.09						28.80	49.28	0.01	32.57	0.67	0.00	0.15	16.00	2.28	0.02	0.00	0.00	0.00	100.97
050424-071	Clot-1	PR	49.19	50.06	0.75						18.82	56.40	0.09	27.40	0.99	0.00	0.13	10.16	5.72	0.13	0.00	0.00	0.00	101.01
050424-072	Clot-1	PC	70.95	28.95	0.10						48.65	51.13	0.00	31.34	0.59	0.00	0.31	14.46	3.26	0.02	0.00	0.00	0.00	101.11
050424-073	Clot-1	PR	62.13	37.45	0.42						12.94	53.46	0.01	30.04	0.79	0.00	0.07	12.91	4.30	0.07	0.00	0.00	0.00	101.65
050424-078	Clot-1	PC	79.02	20.95	0.03						33.71	48.43	0.00	32.31	0.53	0.00	0.15	16.07	2.35	0.01	0.00	0.00	0.00	99.85
050424-079	Clot-1	PR	66.74	32.91	0.35						10.66	52.05	0.04	30.75	0.87	0.00	0.06	13.70	3.74	0.06	0.00	0.00	0.00	101.26
050424-080	Clot-1	PC	79.11	20.82	0.08						23.67	48.64	0.00	32.96	0.60	0.00	0.10	16.19	2.36	0.01	0.00	0.00	0.00	100.87
050424-081	Clot-1	PR	60.24	39.46	0.30						17.38	53.85	0.05	29.34	0.94	0.00	0.11	12.50	4.53	0.05	0.00	0.00	0.00	101.37
050424-082	Clot-1	PC	78.86	21.13	0.01						33.65	49.03	0.01	32.49	0.55	0.00	0.16	16.19	2.40	0.00	0.00	0.00	0.00	100.83
050424-083	Clot-1	PR	59.66	40.04	0.30						21.03	52.38	0.06	29.58	0.88	0.00	0.13	12.47	4.63	0.05	0.00	0.00	0.00	100.17

Table T3 (continued).

Analysis number	Mode	Normalized mineral percentages									Major element oxide (wt%)													
		An	Ab	Or	Wo	En	Fs	YAl	YCr	YFe	Mg#	SiO ₂	TiO ₂	Al ₂ O ₃	FeO*	MnO	MgO	CaO	Na ₂ O	K ₂ O	Cr ₂ O ₃	NiO	V ₂ O ₃	Total
050424-084	Clot-1	PC	79.25	20.72	0.04						25.19	48.16	0.00	32.84	0.67	0.00	0.13	15.93	2.30	0.01	0.00	0.00	0.00	100.03
050424-085	Clot-1	PR	67.20	32.54	0.26						19.92	51.34	0.03	30.70	0.82	0.00	0.11	13.87	3.71	0.05	0.00	0.00	0.01	100.63
050424-086	Clot-1	PC	77.26	22.63	0.11						23.01	48.81	0.00	31.93	0.68	0.00	0.11	15.66	2.54	0.02	0.00	0.00	0.00	99.75
050424-087	Clot-1	PR	76.74	23.15	0.10						13.70	48.74	0.00	31.72	0.73	0.00	0.07	15.90	2.65	0.02	0.00	0.00	0.00	99.82
050424-097	Clot-2	PC	77.89	22.07	0.04						37.38	48.47	0.00	32.57	0.47	0.00	0.16	15.89	2.49	0.01	0.01	0.00	0.02	100.08
050424-098	Clot-2	PR	54.60	44.92	0.49						17.30	54.21	0.03	27.90	1.02	0.00	0.12	11.33	5.15	0.09	0.00	0.00	0.00	99.84
050424-099	Clot-2	PC	65.34	34.43	0.23						18.02	51.16	0.02	30.10	0.86	0.00	0.11	13.38	3.90	0.04	0.00	0.00	0.00	99.57
050424-100	Clot-2	PR	54.34	44.96	0.70						17.68	54.33	0.07	27.60	1.88	0.00	0.23	11.10	5.08	0.12	0.00	0.00	0.00	100.40
050424-103	Clot-3	PC	49.58	49.09	1.33						11.38	55.33	0.09	26.62	1.26	0.00	0.09	10.15	5.56	0.23	0.00	0.00	0.00	99.33
050424-104	Clot-3	GC	52.18	47.06	0.76						14.17	55.39	0.01	27.74	1.06	0.00	0.10	10.82	5.39	0.13	0.00	0.00	0.00	100.64
050424-105	Clot-3	PC	67.98	31.92	0.10						32.42	52.39	0.02	30.32	0.68	0.00	0.18	13.96	3.62	0.02	0.00	0.00	0.00	101.21
050424-106	Clot-3	PR	54.99	44.35	0.65						13.88	55.41	0.02	27.95	0.73	0.00	0.07	11.32	5.05	0.11	0.00	0.00	0.00	100.66
050424-111	Vein-1	VC	50.50	49.13	0.37						17.64	55.79	0.02	28.04	0.52	0.00	0.06	10.57	5.68	0.07	0.00	0.00	0.00	100.75
050424-112	Vein-1	VR	52.86	46.64	0.50						25.72	54.79	0.07	27.35	1.29	0.00	0.25	11.02	5.37	0.09	0.00	0.00	0.00	100.22
050424-113		GC	55.21	44.30	0.50						15.15	54.08	0.06	27.73	1.39	0.00	0.14	11.55	5.12	0.09	0.00	0.00	0.00	100.16
050424-114		GC	48.84	49.91	1.25						9.54	55.36	0.15	27.11	1.34	0.00	0.08	10.22	5.77	0.22	0.00	0.00	0.00	100.25
050424-116		GC	54.69	44.31	0.99						6.11	55.46	0.06	28.56	1.04	0.00	0.04	11.34	5.08	0.17	0.00	0.00	0.00	101.75
050424-121		GC	53.16	45.99	0.85						49.82	55.93	0.09	25.38	2.10	0.03	1.17	11.37	5.44	0.15	0.00	0.00	0.00	101.66
<i>Clinopyroxene</i>																								
050424-067	Clot-1	GC		36.78	39.00	24.22					61.70	51.02	0.63	1.25	14.46	0.36	13.06	17.14	0.22	0.01	0.02	0.02	0.09	98.27
050424-068	Clot-1	GC		3.89	50.34	45.78					52.37	51.16	0.15	0.43	26.98	0.62	16.64	1.79	0.06	0.03	0.00	0.00	0.06	97.91
050424-069	Clot-1	GC		37.26	38.38	24.36					61.17	51.41	0.54	1.21	14.64	0.35	12.94	17.48	0.24	0.02	0.02	0.00	0.10	98.95
050424-074	Clot-1	PC		38.82	50.25	10.93					88.213	54.00	0.28	1.87	6.80	0.20	17.55	18.86	0.19	0.00	0.08	0.00	0.03	99.86
050424-075	Clot-1	PR		38.56	39.51	21.93					64.32	51.50	0.65	1.46	13.17	0.37	13.32	18.08	0.22	0.00	0.16	0.00	0.07	99.00
050424-076	Clot-1	PC		38.41	50.72	10.88					82.34	52.29	0.29	1.85	6.88	0.21	18.00	18.97	0.19	0.01	0.16	0.00	0.03	98.88
050424-077	Clot-1	PR		36.83	41.67	21.50					65.97	51.25	0.52	1.41	12.94	0.34	14.07	17.30	0.22	0.01	0.12	0.00	0.07	98.25
050424-091	Pod-1	VC		8.79	51.08	40.13					56.01	52.25	0.44	0.61	23.97	0.65	17.11	4.10	0.08	0.01	0.03	0.00	0.05	99.29
050424-092	Pod-1	VC		9.22	47.63	43.15					52.47	51.57	0.38	0.57	25.45	0.68	15.76	4.24	0.08	0.01	0.00	0.00	0.04	98.78
050424-101	Clot-3	GC		8.28	51.75	39.96					56.43	49.88	0.36	0.57	24.05	0.58	17.47	3.89	0.05	0.02	0.01	0.00	0.05	96.94
050424-102	Clot-3	PC		32.95	38.96	28.09					58.12	49.47	0.55	1.21	16.56	0.40	12.89	15.17	0.21	0.04	0.00	0.00	0.07	96.56
050424-115		GC		37.06	36.00	26.94					57.20	49.24	1.31	2.30	15.75	0.40	11.81	16.92	0.25	0.01	0.01	0.00	0.12	98.11
050424-117		GC		37.40	39.22	23.38					62.66	51.47	0.74	1.38	14.00	0.38	13.18	17.48	0.22	0.00	0.00	0.01	0.07	98.95
050424-118		GC		38.97	36.17	24.86					59.27	50.85	0.67	1.34	14.69	0.36	11.99	17.97	0.21	0.00	0.00	0.00	0.09	98.19
050424-120		GC		37.27	38.51	24.22					61.39	51.72	0.73	1.36	14.47	0.35	12.90	17.38	0.21	0.00	0.01	0.00	0.07	99.20
050424-119							2.55	0.31	97.14	0.58	0.12	9.10	0.94	56.03	29.44	0.26	0.26	0.18	0.04	0.04	0.17	0.15	1.23	
<i>C: 206-1256C-11R-7, 96–100 cm</i>																								
<i>Plagioclase</i>																								
050424-013	Clot-1	PC	69.11	30.76	0.13						36.87	51.30	0.06	31.24	0.64	0.00	0.21	14.39	3.54	0.02	0.00	0.01	0.03	101.45
050424-015	Clot-1	PC	72.96	26.91	0.13						36.88	49.47	0.01	31.10	0.60	0.00	0.20	15.09	3.08	0.02	0.00	0.00	0.00	99.57
050424-016	Clot-1	PR	72.09	27.75	0.16						36.57	50.35	0.01	31.35	0.60	0.00	0.19	14.87	3.16	0.03	0.00	0.00	0.00	100.55
050424-017	Clot-1	PC	70.92	28.99	0.09						29.13	51.32	0.01	31.13	0.67	0.00	0.15	14.63	3.31	0.02	0.00	0.00	0.00	101.23
050424-018	Clot-1	PR	66.14	33.63	0.23						15.58	51.99	0.05	30.44	0.89	0.00	0.09	13.86	3.90	0.04	0.00	0.00	0.00	101.26
050424-019	Clot-2	PC	71.86	28.03	0.11						39.33	50.61	0.02	30.93	0.58	0.00	0.21	14.79	3.19	0.02	0.00	0.00	0.00	100.35
050424-020	Clot-2	PR	68.29	31.37	0.34						15.74	50.98	0.02	29.91	0.92	0.00	0.10	14.23	3.61	0.06	0.02	0.00	0.00	99.85
050424-021	Clot-2	PC	71.09	28.74	0.17						37.13	50.77	0.02	31.18	0.63	0.00	0.21	14.72	3.29	0.03	0.00	0.00	0.00	100.84
050424-022	Clot-2	PR	70.59	29.26	0.15						24.98	50.75	0.00	31.48	0.73	0.00	0.14	14.72	3.37	0.03	0.00	0.00	0.00	101.21

Table T3 (continued).

Analysis number	Mode	Normalized mineral percentages									Major element oxide (wt%)													
		An	Ab	Or	Wo	En	Fs	YAl	YCr	YFe	Mg#	SiO ₂	TiO ₂	Al ₂ O ₃	FeO*	MnO	MgO	CaO	Na ₂ O	K ₂ O	Cr ₂ O ₃	NiO	V ₂ O ₃	Total
050424-023	Clot-2	PC	69.94	29.88	0.18						35.12	50.99	0.01	30.85	0.67	0.00	0.20	14.41	3.40	0.03	0.01	0.00	0.00	100.58
050424-024	Clot-2	PR	51.72	47.07	1.21						20.32	55.47	0.04	27.86	0.94	0.00	0.13	10.84	5.45	0.21	0.00	0.00	0.00	100.95
050424-025	Clot-2	PC	72.36	27.50	0.14						38.02	50.17	0.00	30.26	0.62	0.00	0.21	14.85	3.12	0.02	0.00	0.00	0.00	99.25
050424-026	Clot-2	PR	53.27	45.75	0.97						18.09	55.21	0.05	27.76	1.15	0.00	0.14	11.14	5.29	0.17	0.00	0.00	0.00	100.90
050424-027	Discrete	PC	73.58	26.31	0.11						38.06	50.66	0.02	31.39	0.59	0.01	0.20	15.22	3.01	0.02	0.00	0.00	0.00	101.11
050424-028	Discrete	PR	66.81	33.08	0.11						17.35	52.17	0.04	31.26	0.86	0.00	0.10	14.05	3.84	0.02	0.00	0.00	0.00	102.34
050424-047	Discrete	MC	71.32	28.59	0.08						31.24	50.76	0.02	29.99	0.68	0.00	0.17	14.65	3.25	0.01	0.00	0.00	0.00	99.53
050424-048	Discrete	MR	55.29	43.98	0.73						12.76	53.85	0.04	27.46	0.79	0.00	0.07	11.40	5.01	0.13	0.00	0.00	0.00	98.75
050424-050	Discrete	PC	72.63	27.26	0.11						33.31	50.32	0.01	30.52	0.70	0.00	0.20	15.19	3.15	0.02	0.00	0.00	0.00	100.09
050424-051	Discrete	PR	77.38	22.52	0.09						16.35	49.38	0.00	31.67	0.81	0.00	0.09	15.90	2.56	0.02	0.00	0.00	0.00	100.42
050424-052	Discrete	PC	69.44	30.48	0.08						36.47	52.01	0.00	30.65	0.64	0.00	0.21	14.56	3.53	0.01	0.00	0.00	0.00	101.62
050424-053	Discrete	PR	75.22	24.65	0.13						20.69	49.21	0.00	31.98	0.75	0.00	0.11	15.45	2.80	0.02	0.00	0.00	0.00	100.31
050424-029	GC	56.62	42.95	0.43							14.76	54.06	0.05	28.36	1.31	0.00	0.13	11.73	4.92	0.07	0.00	0.00	0.00	100.64
050424-031	GC	55.57	43.99	0.44							16.63	54.75	0.06	27.98	1.42	0.00	0.16	11.68	5.11	0.08	0.00	0.00	0.00	101.23
050424-032	GC	56.75	42.68	0.57							16.39	54.69	0.07	27.94	1.61	0.00	0.18	11.79	4.90	0.10	0.00	0.00	0.00	101.27
050424-033	GC	56.07	43.37	0.56							12.44	53.65	0.07	28.51	1.09	0.00	0.09	11.66	4.98	0.10	0.00	0.00	0.00	100.14
050424-034	GC	56.52	43.11	0.36							19.29	53.92	0.10	27.49	1.57	0.00	0.21	11.64	4.91	0.06	0.00	0.00	0.00	99.90
050424-035	GC	56.21	43.35	0.45							17.31	54.08	0.08	27.71	1.38	0.00	0.16	11.73	5.00	0.08	0.00	0.00	0.00	100.21
050424-036	GC	57.41	42.07	0.53							16.36	54.37	0.06	27.72	1.46	0.00	0.16	11.93	4.83	0.09	0.01	0.00	0.00	100.63
050424-037	GC	52.39	46.71	0.90							25.07	55.52	0.07	27.80	1.04	0.00	0.20	10.95	5.39	0.16	0.00	0.00	0.00	101.11
050424-038	GC	56.46	42.87	0.67							14.82	54.06	0.07	27.37	1.67	0.00	0.16	11.78	4.94	0.12	0.00	0.00	0.00	100.16
050424-039	GC	54.90	44.51	0.59							12.84	54.65	0.02	28.35	0.93	0.00	0.08	11.36	5.09	0.10	0.00	0.00	0.00	100.59
050424-040	GC	50.20	48.90	0.90							15.27	55.84	0.09	27.88	1.24	0.00	0.13	10.77	5.80	0.16	0.00	0.00	0.00	101.89
050424-042	GC	50.91	47.79	1.29							8.48	54.76	0.05	27.34	1.21	0.00	0.06	10.64	5.52	0.23	0.00	0.00	0.00	99.80
050613-049	NC	52.31	46.38	1.30							4.34	55.50	0.01	27.19	0.94	0.00	0.02	10.62	5.20	0.22	0.00	0.00	0.00	99.70
050613-051	NC	50.55	48.20	1.25							26.42	55.79	0.01	26.57	1.12	0.00	0.23	10.42	5.49	0.22	0.00	0.00	0.00	99.85
050613-052	NC	51.32	47.64	1.04							12.27	54.41	0.05	26.67	1.36	0.00	0.11	10.52	5.40	0.18	0.00	0.00	0.00	98.69
<i>Clinopyroxene</i>																								
050424-014	Clot-1	PR				36.14	38.60	25.27			60.44	49.98	0.68	1.31	15.43	0.40	13.22	17.23	0.23	0.00	0.01	0.00	0.01	98.50
050424-041	GC					38.05	37.75	24.20			60.94	50.98	0.71	1.35	14.80	0.38	12.95	18.16	0.23	0.01	0.02	0.00	0.03	99.62
050424-043	GC					37.82	38.03	24.16			61.15	51.52	0.54	1.13	14.80	0.38	13.07	18.08	0.24	0.00	0.00	0.01	0.03	99.80
050424-044	GC					38.17	33.93	27.89			54.89	48.39	1.22	2.02	16.77	0.32	11.45	17.91	0.25	0.01	0.05	0.00	0.02	98.41
050424-045	GC					37.75	36.21	26.04			58.17	50.84	0.63	1.35	15.61	0.37	12.18	17.66	0.24	0.01	0.00	0.00	0.04	98.93
050424-046	GC					38.88	35.02	26.10			57.29	76.67	0.31	0.53	8.06	0.17	6.07	9.37	0.15	0.01	0.01	0.00	0.01	101.37
050424-049	GC					4.74	47.94	47.32			50.33	51.79	0.16	0.38	28.51	0.59	16.20	2.23	0.03	0.02	0.00	0.00	0.06	99.96
050424-055	MR					40.84	35.67	23.49			60.29	51.28	0.73	3.97	13.00	0.30	11.07	17.64	0.68	0.03	0.04	0.00	0.03	98.77
050424-056	GC					39.39	37.92	22.70			62.56	51.06	0.50	1.11	13.92	0.39	13.05	18.86	0.24	0.00	0.04	0.00	0.06	99.22
050613-045	NC					35.95	39.43	24.62			61.57	49.06	0.69	1.33	15.29	0.40	13.74	17.43	0.20	0.01	0.01	0.01	0.03	98.21
050613-048	NC					37.69	36.95	25.36			59.30	51.25	0.84	1.61	15.64	0.35	12.78	18.14	0.28	0.00	0.00	0.05	0.05	100.95
050613-050	NC					37.23	38.28	24.49			60.99	51.26	0.61	1.26	14.97	0.40	13.13	17.77	0.19	0.01	0.01	0.04	0.04	99.66
050424-054	GC					4.38	0.51	95.11	15.75	19.04	7.75	1.36	46.39	17.95	0.25	6.26	5.69	0.16	0.05	0.24	0.09	0.73		

Notes: VC = vein core, VR = vein rim, PC = phenocryst core, PR = phenocryst rim, GC = core of a crystal in the groundmass, GR = rim of a crystal in the groundmass, MC = microphenocryst core, MR = microphenocryst rim, NC = neoblast core. YAl = Al/(Al + Cr + Fe³⁺), YCr = Cr/(Al + Cr + Fe³⁺), YFe = Fe³⁺/(Al + Cr + Fe³⁺), Mg# = 100 × Mg/(Mg + Fe), FeO* = Fe as total FeO.